Resonance-assisted tunneling in mixed regular-chaotic systems

Peter Schlagheck, Amaury Mouchet, Denis Ullmo

Chapter 8

Resonance-assisted tunneling in mixed regular-chaotic systems

Peter Schlagheck[1], Amaury Mouchet[2], and Denis Ullmo[3]

[1] Département de Physique, Université de Liège, 4000 Liège, Belgium
[2] Laboratoire de Mathématiques et de Physique Théorique, Université François Rabelais de Tours — CNRS (UMR 6083), Fédération Denis Poisson, Parc de Grandmont, 37200 Tours, France
[3] LPTMS UMR 8626, Univ. Paris-Sud, CNRS, 91405 Orsay Cedex, France

8.1 Introduction

8.1.1 Tunneling in integrable systems

Since the early days of quantum mechanics, tunneling has been recognized as one of the hallmarks of the wave character of microscopic physics. The possibility of a quantum particle to penetrate an energetic barrier represents certainly one of the most spectacular implications of quantum theory and has lead to various applications in nuclear, atomic and molecular physics as well as in mesoscopic science. Typical scenarios in which tunneling manifests are the escape of a quantum particle from a quasi-bounded region, the transition between two or more symmetry-related, but classically disconnected wells (which we shall focus on in the following), as well as scattering or transport through potential barriers. The spectrum of scenarios becomes even richer when the concept of tunneling is generalized to any kind of classically forbidden transitions in phase space, i.e. to transitions that are not necessarily inhibited by static potential barriers but by some other constraints of the underlying classical dynamics (such as integrals of motion). Such "dynamical tunneling" processes arise frequently in molecular systems [1] and were realized with cold atoms propagating in periodically modulated optical lattices [2, 3, 4]. Moreover, the electromagnetic analog of dynamical

tunneling was also obtained with microwaves in billiards [5].

Despite its genuinely quantal nature, tunneling is strongly influenced by the structure of the underlying classical phase space (see Ref. [6] for a review). This is best illustrated within the textbook example of a one-dimensional symmetric double-well potential. In this simple case, the eigenvalue problem can be straightforwardly solved with the standard Jeffreys-Wentzel-Kramers-Brillouin (JWKB) ansatz [7]. The eigenstates of this system are, below the barrier height, obtained by the symmetric and antisymmetric linear combination of the local "quasi-modes" (i.e., of the wave functions that are semiclassically constructed on the quantized orbits within each well, without taking into account the classically forbidden coupling between the wells), and the splitting of their energies is given by an expression of the form

$$\Delta E = \frac{\hbar\Omega}{\pi} \exp\left[-\frac{1}{\hbar}\int \sqrt{2m(V(x)-E)}dx\right] . \tag{8.1}$$

Here E is the mean energy of the doublet, $V(x)$ represents the double well potential, m is the mass of the particle, Ω denotes the oscillation frequency within each well, and the integral in the exponent is performed over the whole classically forbidden domain, i.e. between the inner turning points of the orbits in the two wells. Preparing the initial state as one of the quasi-modes (i.e., as the even or odd superposition of the symmetric and the antisymmetric eigenstate), the system will undergo Rabi oscillations between the wells with the frequency $\Delta E/\hbar$. The "tunneling rate" of this system is therefore given by the splitting (8.1). Keeping all classical parameters fixed, it decreases exponentially with $1/\hbar$, and, in that sense, one can say that tunneling "vanishes" in the classical limit.

8.1.2 Chaos-assisted tunneling

The approach presented in the previous section can be generalized to multidimensional, even non-separable systems, as long as their classical dynamics is still integrable [8]. It breaks down, however, as soon as a non-integrable perturbation is added to the system, e.g. if the one-dimensional double-well potential is exposed to a driving that is periodic in time (with period τ, say). In that case, the classical phase space of the system generally becomes a mixture of both regular and chaotic structures.

As visualized by the stroboscopic Poincaré section — which is obtained by retaining the phase space coordinates at every integer multiple of the driving period τ — the phase space typically displays two prominent regions of regular motion, corresponding to the weakly perturbed dynamics within the two wells, and a small (or, for stronger perturbations, large) layer of chaotic dynamics that separates the two regular islands from each other. Numerical calculations of model systems in the early nineties [9, 10] have shown that the tunnel splittings in such mixed systems generally become strongly enhanced compared to the integrable limit. Moreover, they do no longer follow a smooth exponential scaling with $1/\hbar$ as expressed by Eq. (8.1), but display huge, quasi-erratic fluctuations when $\hbar$ or any other parameter of the system vary [9, 10].

These phenomena are traced back to the specific role that *chaotic* states play in such systems [11, 12, 13, 14]. In contrast to the integrable case, the tunnel doublets of the localized quasi-modes are, in a mixed regular-chaotic system, no longer isolated in the spectrum, but resonantly interact with states that are associated with the chaotic part of phase space. Due

to their delocalized nature in phase space[1], such chaotic states typically exhibit a significant overlap with the boundary regions of both regular wells. Therefore, they may provide an efficient coupling mechanism between the quasi-modes – which becomes particularly effective whenever one of the chaotic levels is shifted exactly on resonance with the tunnel doublet. As illustrated in Fig. 8.1, this coupling mechanism generally enhances the tunneling rate, but may also lead to a complete suppression thereof, arising at specific values of $\hbar$ or other parameters [16].

We point out that this type of resonant tunneling does not necessarily require the presence of classical chaos and may appear also in integrable systems, for instance in a one-dimensional symmetric triple-well potential. This is illustrated in Fig. 8.2, which shows the scaling of level splittings associated with the two lateral wells as a function of $1/\hbar$ for such a triple-well potential. On top of an exponential decrease according to Eq. (8.1), the splittings display strong spikes occuring whenever the energy of a state localized in the central well becomes quasi-degenerate with the energies of the states in the two lateral wells.

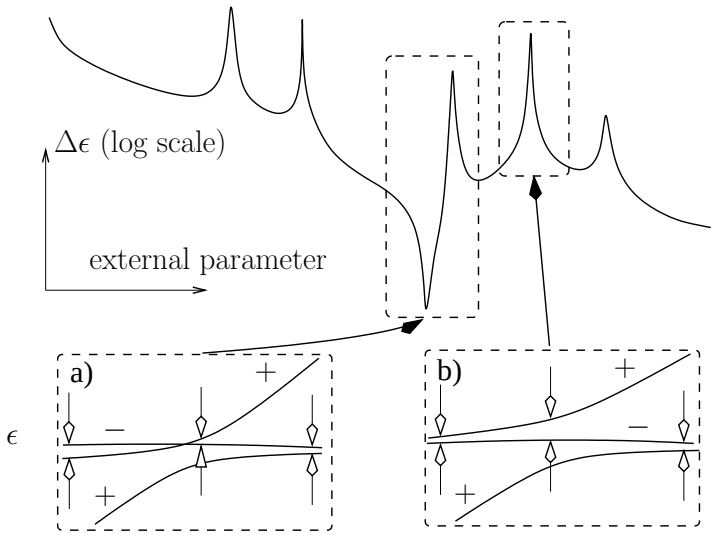

Figure 8.1: The two elementary scenarios of huge enhancement (case b) or cancellation (case a) of the tunneling splitting between symmetric (+) and anti-symmetric (−) states can be easily understood from the resonant crossing of a third level (here a symmetric one) and the corresponding level repulsion between states of the same symmetry class. The external parameter that triggers the fluctuation of tunneling can be of quantum origin (effective $\hbar$) or classical.

For mixed regular-chaotic systems, the validity of this "chaos-assisted" tunneling picture was essentially confirmed by successfully modeling the chaotic part of the quantum dynamics with a random matrix from the Gaussian orthogonal ensemble (GOE) [11, 12, 17]. Using the fact that the coupling coefficients between the regular states and the chaotic domain are small, this random matrix ansatz yields a truncated Cauchy distribution for the probability density to obtain a level splitting of the size ΔE. Such a distribution is indeed encountered in the exact quantum splittings, which was demonstrated for the two-dimensional quartic oscillator [17] as well as, later on, for the driven pendulum Hamiltonian that describes

[1]We assume here that the effects of dynamical localization observed in Ref. [15] remain irrelevant.

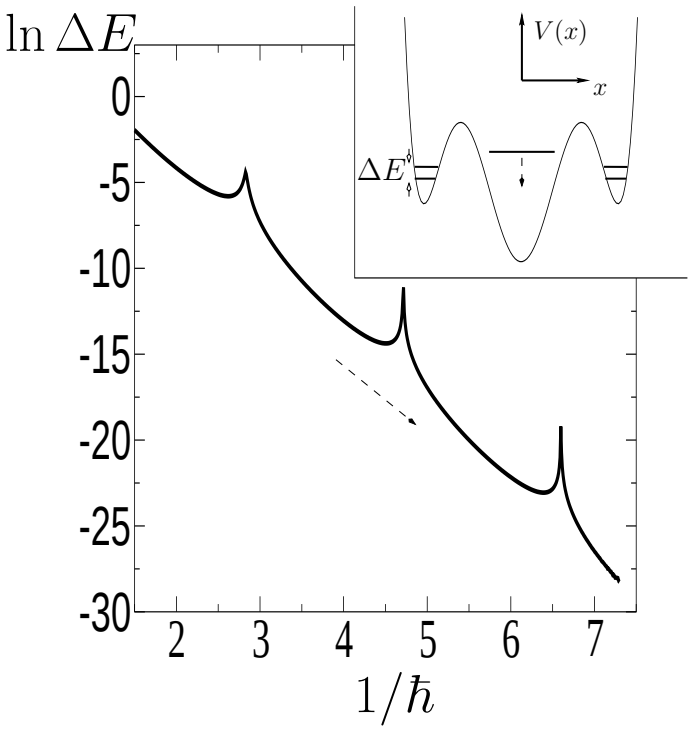

Figure 8.2: Resonant tunneling at work for a one dimensional triple well potential (here $V(x) = (x^2 - a^2)^2(x^2 - b^2)$ with $a = 1.75$ and $b = .5$). When $1/\hbar$ is increased, tunneling between the two lateral wells is enhanced by several orders of magnitude each time a level in the central well crosses down the doublet.

the tunneling process of cold atoms in periodically modulated optical lattices [4, 18]. A quantitative prediction of the *average* tunneling rate, however, was not possible in the above-mentioned theoretical works. As we shall argue later on, this average tunneling rate is directly connected to the coupling matrix element between the regular and the chaotic states, and the strength of this matrix element was unknown and introduced in an ad-hoc way.

A first step towards this latter problem was undertaken by Podolskiy and Narimanov [19] who proposed an explicit semiclassical expression for the mean tunneling rate in a mixed system by assuming a perfectly clean, harmonic-oscillator like dynamics within the regular island and a structureless chaotic sea outside the outermost invariant torus of the island. This expression turned out to be successful for the reproduction of the level splittings between near-degenerate optical modes that are associated with a pair of symmetric regular islands in a non-integrable micro-cavity [19] (see also Ref. [20]). The application to dynamical tunneling in periodically modulated optical lattices [19], for which splittings between the left- and the right-moving stable eigenmodes were calculated in Ref. [4], seems convincing for low and moderate values of $1/\hbar$, but reveals deviations deeper in the semiclassical regime where plateau structures arise in the tunneling rates. Further, and more severe, deviations were encountered in the application of this approach to tunneling processes in other model systems [21].

Bäcker, Ketzmerick, Löck, and coworkers [22, 23] recently undertook the effort to derive more rigorously the regular-to-chaotic coupling rate governing chaos-assisted tunneling. Their approach is based on the construction of an integrable approximation for the nonintegrable system, designed to accurately describe the motion within the regular islands under consideration. The coupling rate to the chaotic domain is then determined through the computation of matrix elements of the Hamiltonian of the system within the eigenbasis of this integrable approximation [22]. This results in a smooth exponential-like decay of the average tunneling rate with $1/\hbar$, which was indeed found to be in very good agreement with the exact tunneling rates for quantum maps and billiards [22, 23]. Those systems, however, were designed such as to yield a "clean" mixed regular-chaotic phase space, containing a regular island and a chaotic region which both do not exhibit appreciable substructures [22, 23].

8.1.3 The role of nonlinear resonances

In more generic systems, such as the quantum kicked rotor or the driven pendulum [4], however, even the "average" tunneling rates do not exhibit a smooth monotonous behaviour with $1/\hbar$, but display peaks and plateau structures that cannot be accounted for by the above approaches. To understand the origin of such plateaus, it is instructive to step back to the conceptually simpler case of *nearly integrable* dynamics, where the perturbation from the integrable Hamiltonian is sufficiently small such that macroscopically large chaotic layers are not yet developed in the Poincaré surface of section. In such systems, the main classical phase space features due to the perturbation consist in chain-like substructures that surround stable periodic orbits or equilibrium points of the classical motion. Those substructures come from *nonlinear resonances* between the internal degrees of freedom of the system or, for driven systems, between the external driving and the unperturbed oscillations around the central orbit. In a similar way as for the quantum pendulum Hamiltonian, such resonances induce additional tunneling paths in the phase space, which lead to couplings between states that are located near the *same* stable orbit [24, 25].

The relevance of this effect for the near-integrable tunneling process between two symmetry-related wells was first pointed out by Bonci et al. [26] who argued that such resonances may lead to a strong enhancement of the tunneling rate, due to couplings between lowly and highly excited states within the well which are permitted by near-degeneracies in the spectrum In Refs. [27, 28], a quantitative semiclassical theory of near-integrable tunneling was formulated on the basis of this principal mechanism. This theory allows one to reproduce the exact quantum splittings from purely classical quantities and takes into account high-order effects such as the coupling via a sequence of different resonance chains [27, 28]. More recent studies by Keshavamurthy on classically forbidden coupling processes in model systems that mimic the dynamics of simple molecules confirm that the resonance-assisted tunneling scenario prevails not only in one-dimensional systems that are subject to a periodic driving (such as the kicked Harper model studied in Ref. [27, 28]), but also in autonomous systems with two and even three degrees of freedom [29, 30].

In Refs. [31, 32, 33, 34] resonance-assisted couplings were incorporated in an approximate manner into the framework of chaos-assisted tunneling in order to provide a quantitative theory for the regular-to-chaotic coupling rate. In this context, it is assumed that the dominant coupling between regular states within and chaotic states outside the island is provided by the presence of a nonlinear resonance within the island. A straightforward implementation of this idea yields good agreement with the exact tunneling rates as far as their average decay with $1/\hbar$ in the deep semiclassical limit is concerned. Moreover, individual plateaus

and peak structures could be traced back to the influence of specific nonlinear resonances, not only for double-well-type tunneling in closed or periodic systems [31, 32, 33], but also for tunneling-induced decay in open systems [34]. However, the predictive power of this method was still rather limited, insofar as individual tunneling rates at given system parameters could be over- or underestimated by many orders of magnitude. In particular, resonance-assisted tunneling seemed inapplicable in the "quantum" limit of large $\hbar$, where direct regular-to chaotic tunneling proved successful [22, 23].

A major advance in this context was achieved by improving the semiclassical evaluation of resonance-induced coupling processes in mixed systems, and by combining it with "direct" regular-to-chaotic tunneling [35]. This combination resulted, for the first time, in a semiclassical prediction of tunneling rates in generic mixed regular-chaotic systems that can be compared with the exact quantum rates on the level of individual peak structures [35]. This confirms the expectation that nonlinear resonances do indeed form the "backbone" behind non-monotonous substructures in tunneling rates. It furthermore suggests that those rates could, also in systems with more degrees of freedom, possibly be estimated in a quantitatively satisfactory manner via simple classical computations, based on the most prominent nonlinear resonances that are manifested within the regular island.

It is in the spirit of this latter expectation that this contribution has been written. Our aim is not to formulate a formal semiclassical theory of tunneling in mixed systems, which still represents an open problem that would rather have to be solved on the basis of complex classical orbits [36, 37, 38]. Instead, we want to provide a simple, easy-to-implement, yet effective prescription how to compute the rates and time scales associated with tunneling processes solely on the basis of the classical dynamics of the system, without performing any diagonalization (not even any application) of the quantum Hamiltonian or of the time evolution operator. This prescription is based on chaos- and resonance-assisted tunneling in its improved form [35]. The main part of this contribution is therefore devoted to a detailed description of resonance-assisted tunneling and its combination with chaos-assisted tunneling in the sections 8.2 and 8.3, respectively. We present in section 8.4 the application of this method to tunneling processes in the quantum kicked rotor, and discuss possible limitations and future prospects in the conclusion in section 8.5.

8.2 Theory of resonance-assisted tunneling

8.2.1 Secular perturbation theory

For our study, we restrict ourselves to systems with one degree of freedom that evolve under a periodically time-dependent Hamiltonian $H(p, q, t) = H(p, q, t + \tau)$. We suppose that, for a suitable choice of parameters, the classical phase space of H is mixed regular-chaotic and exhibits two symmetry-related regular islands that are embedded within the chaotic sea. This phase space structure is most conveniently visualized by a stroboscopic Poincaré section, where p and q are plotted at the times $t = n\tau (n \in \mathbb{Z})$. Such a Poincaré section typically reveals the presence of chain-like substructures within the regular islands, which arise due to nonlinear resonances between the external driving and the internal oscillation around the island's center. Before considering the general situation for which many resonances may come into play in the tunneling process, we start with the simpler case where the two islands exhibit a prominent r:s resonance, i.e., a nonlinear resonance where s internal oscillation

periods match r driving periods and r sub-islands are visible in the stroboscopic section.

The classical motion in the vicinity of the r:s resonance is approximately integrated by secular perturbation theory [39] (see also Ref. [28]). For this purpose, we formally introduce a time-independent Hamiltonian $H_0(p,q)$ that approximately reproduces the regular motion in the islands and preserves the discrete symmetry of H. In some circumstances, as for instance if H is in the nearly integrable regime, $H_0(p,q)$ can be explicitly computed within some approximation scheme (using for instance the Lie transformation method [39]). We stress though that this will not always be necessary. Assuming the existence of such a H_0, the phase space generated by this integrable Hamiltonian consequently exhibits two symmetric wells that are separated by a dynamical barrier and "embed" the two islands of H. In terms of the action-angle variables (I,θ) describing the dynamics within each of the wells, the total Hamiltonian can be written as

$$H(I,\theta,t) = H_0(I) + V(I,\theta,t) \tag{8.2}$$

where V would represent a weak perturbation in the center of the island [2]

The nonlinear r:s resonance occurs at the action variable $I_{r:s}$ that satisfies the condition

$$r\Omega_{r:s} = s\omega \tag{8.3}$$

with $\omega = 2\pi/\tau$ and

$$\Omega_{r:s} \equiv \left.\frac{dH_0}{dI}\right|_{I=I_{r:s}} . \tag{8.4}$$

We now perform a canonical transformation to the frame that corotates with this resonance. This is done by leaving I invariant and modifying θ according to

$$\theta \mapsto \vartheta = \theta - \Omega_{r:s}t\,. \tag{8.5}$$

This time-dependent shift is accompanied by the transformation $H \mapsto \mathcal{H} = H - \Omega_{r:s}I$ in order to ensure that the new corotating angle variable ϑ is conjugate to I. The motion of I and ϑ is therefore described by the new Hamiltonian

$$\mathcal{H}(I,\vartheta,t) = \mathcal{H}_0(I) + \mathcal{V}(I,\vartheta,t) \tag{8.6}$$

with

$$\mathcal{H}_0(I) = H_0(I) - \Omega_{r:s}I\,, \tag{8.7}$$
$$\mathcal{V}(I,\vartheta,t) = V(I,\vartheta+\Omega_{r:s}t,t)\,. \tag{8.8}$$

The expansion of $\mathcal{H}_0$ in powers of $I - I_{r:s}$ yields

$$\mathcal{H}_0(I) \simeq \mathcal{H}_0^{(0)} + \frac{(I-I_{r:s})^2}{2m_{r:s}} + \mathcal{O}\left[(I-I_{r:s})^3\right] \tag{8.9}$$

with a constant $\mathcal{H}_0^{(0)} \equiv H_0(I_{r:s}) - \Omega_{r:s}I_{r:s}$ and a quadratic term that is characterized by the effective "mass" parameter $m_{r:s} \equiv [d^2H_0/dI^2(I_{r:s})]^{-1}$. Hence, $d\mathcal{H}_0/dI$ is comparatively small for $I \simeq I_{r:s}$, which implies that the co-rotating angle ϑ varies slowly in time near

[2] In order not to overload the notation, we use the same symbol H for the Hamiltonian in the original phase-space variables (p,q) and in the action-angle variables (I,θ).

the resonance. This justifies the application of adiabatic perturbation theory [39], which effectively amounts, in first order, to replacing $\mathcal{V}(I,\vartheta,t)$ by its time average over r periods of the driving (using the fact that $\mathcal{V}$ is periodic in t with the period $r\tau$) [3]. We therefore obtain, after this transformation, the time-independent Hamiltonian

$$\mathcal{H}(I,\vartheta) = \mathcal{H}_0(I) + \mathcal{V}(I,\vartheta) \tag{8.10}$$

with

$$\mathcal{V}(I,\vartheta) \equiv \frac{1}{r\tau}\int_0^{r\tau} \mathcal{V}(I,\vartheta,t)dt\,. \tag{8.11}$$

By expanding $V(I,\theta,t)$ in a Fourier series in both θ and t, i.e.

$$V(I,\theta,t) = \sum_{l,m=-\infty}^{\infty} V_{l,m}(I)e^{il\theta}e^{im\omega t} \tag{8.12}$$

with $V_{l,m}(I) = [V_{-l,-m}(I)]^*$, one can straightforwardly derive

$$\mathcal{V}(I,\vartheta) = V_{0,0}(I) + \sum_{k=1}^{\infty} 2V_k(I)\cos(kr\vartheta + \phi_k) \tag{8.13}$$

defining

$$V_k(I)e^{i\phi_k} \equiv V_{rk,-sk}(I)\,, \tag{8.14}$$

i.e., the resulting time-independent perturbation term is $(2\pi/r)$-periodic in ϑ.

For the sake of clarity, we start discussing the resulting effective Hamiltonian neglecting the action dependence of the Fourier coefficients of $\mathcal{V}(I,\vartheta)$. We stress that this dependence can be implemented in a relatively straightforward way using Birkhoff-Gustavson normal-form coordinates (cf section 8.2.3 below); it is actually important to obtain a good quantitative accuracy. For now, however, we replace $V_k(I)$ by $V_k \equiv V_k(I = I_{r:s})$ in Eq. (8.13). Neglecting furthermore the term $V_{0,0}(I)$, we obtain the effective integrable Hamiltonian

$$H_{\rm res}(I,\vartheta) = H_0(I) - \Omega_{r:s}I + \sum_{k=1}^{\infty} 2V_k\cos(kr\vartheta + \phi_k) \tag{8.15}$$

for the description of the classical dynamics in the vicinity of the resonance. We shall see in section 8.2.2 that the parameters of $H_{\rm res}$ relevant to the tunneling process can be extracted directly from the classical dynamics of $H(t)$, which is making Eq. (8.15) particularly valuable.

8.2.2 The pendulum approximation

The quantum implications due to the presence of this nonlinear resonance can be straightforwardly inferred from the direct semiclassical quantization of $H_{\rm res}$, given by

$$\hat{H}_{\rm res} = H_0(\hat{I}) - \Omega_{r:s}\hat{I} + \sum_{k=1}^{\infty} 2V_k\cos(kr\hat{\vartheta} + \phi_k)\,. \tag{8.16}$$

[3] This step involves, strictly speaking, another time-dependent canonical transformation $(I,\vartheta) \mapsto (\widetilde{I},\widetilde{\vartheta})$ which slightly modifies I and ϑ (see also Ref. [28]).

Here we introduce the action operator $\hat{I} \equiv -i\hbar\partial/\partial\vartheta$ and assume anti-periodic boundary conditions in ϑ in order to properly account for the Maslov index in the original phase space [24]. In accordance with our assumption that the effect of the resonance is rather weak, we can now apply quantum perturbation theory to the Hamiltonian (8.16), treating the $\hat{I}$-dependent "kinetic" terms as unperturbed part and the $\hat{\vartheta}$-dependent series as perturbation. The unperturbed eigenstates are then given by the (anti-periodic) eigenfunctions $\langle\vartheta|n\rangle = (2\pi)^{-1/2}\exp[i(n+1/2)\vartheta]$ $(n \geq 0)$ of the action operator $\hat{I}$ with the eigenvalues

$$I_n = \hbar(n+1/2)\,. \tag{8.17}$$

As is straightforwardly evaluated, the presence of the perturbation induces couplings between the states $|n\rangle$ and $|n+kr\rangle$ with the matrix elements

$$\langle n+kr|\hat{H}_{\rm res}|n\rangle = V_k e^{i\phi_k} \tag{8.18}$$

for strictly positive integer k. As a consequence, the "true" eigenstates $|\psi_n\rangle$ of $\hat{H}_{\rm res}$ contain admixtures from unperturbed modes $|n'\rangle$ that satisfy the selection rule $|n'-n| = kr$ with integer k. They are approximated by the expression

$$\begin{aligned} |\psi_n\rangle &= |n\rangle + \sum_k \frac{\langle n+kr|\hat{H}_{\rm res}|n\rangle}{E_n - E_{n+kr} + ks\hbar\omega}|n+kr\rangle + \\ &\quad + \sum_{k,k'} \frac{\langle n+kr|\hat{H}_{\rm res}|n+k'r\rangle}{E_n - E_{n+kr} + ks\hbar\omega}\frac{\langle n+k'r|\hat{H}_{\rm res}|n\rangle}{E_n - E_{n+k'r} + k's\hbar\omega}|n+kr\rangle + \ldots \end{aligned} \tag{8.19}$$

where $E_n \equiv H_0(I_n)$ denote the unperturbed eigenenergies of H_0 and the resonance condition (8.3) is used. The summations in Eq. (8.19) are generally finite due to the finiteness of the phase space area covered by the regular region.

Within the quadratic approximation of $H_0(I)$ around $I_{r:s}$, we obtain from Eqs. (8.7) and (8.9)

$$E_n \simeq H_0(I_{r:s}) + \Omega_{r:s}(I_n - I_{r:s}) + \frac{1}{2m_{r:s}}(I_n - I_{r:s})^2\,. \tag{8.20}$$

This results in the energy differences

$$E_n - E_{n+kr} + ks\hbar\omega \simeq \frac{1}{2m_{r:s}}(I_n - I_{n+kr})(I_n + I_{n+kr} - 2I_{r:s})\,. \tag{8.21}$$

From this expression, we see that the admixture between $|n\rangle$ and $|n'\rangle$ becomes particularly strong if the r:s resonance is symmetrically located between the two tori that are associated with the actions I_n and $I_{n'}$ — i.e., if $I_n + I_{n'} \simeq 2I_{r:s}$. The presence of a significant nonlinear resonance within a region of regular motion provides therefore an efficient mechanism to couple the local "ground state" — i.e, the state that is semiclassically localized in the center of that region (with action variable $I_0 < I_{r:s}$) — to a highly excited state (with action variable $I_{kr} > I_{r:s}$).

It is instructive to realize that the Fourier coefficients V_k of the perturbation operator decrease rather rapidly with increasing k. Indeed, one can derive under quite general circumstances the asymptotic scaling law

$$V_k \sim (kr)^\gamma V_0 \exp[-kr\Omega_{r:s}t_{\rm im}(I_{r:s})] \tag{8.22}$$

for large k, which is based on the presence of singularities of the complexified tori of the integrable approximation $H_0(I)$ (see Eq. (66) in Ref. [28]). Here $t_{\rm im}(I)$ denotes the imaginary time that elapses from the (real) torus with action I to the nearest singularity in complex phase space, γ corresponds to the degree of the singularity, and V_0 contains information about the corresponding residue near the singularity as well as the strength of the perturbation. The expression (8.22) is of little practical relevance as far as the concrete determination of the coefficients V_k is concerned. It permits, however, to estimate the relative importance of different perturbative pathways connecting the states $|n\rangle$ and $|n+kr\rangle$ in Eq. (8.19). Comparing e.g. the amplitude $\mathcal{A}_2$ associated with a single step from $|n\rangle$ to $|n+2r\rangle$ via V_2 and the amplitude $\mathcal{A}_1$ associated with two steps from $|n\rangle$ to $|n+2r\rangle$ via V_1, we obtain from Eqs. (8.21) and (8.22) the ratio

$$\mathcal{A}_2/\mathcal{A}_1 \simeq \frac{2^{\gamma-1}r^{2-\gamma}\hbar^2}{m_{r:s}V_0}e^{i(\phi_2-2\phi_1)} \tag{8.23}$$

under the assumption that the resonance is symmetrically located in between the corresponding two tori (in which case we would have $I_{n+r} \simeq I_{r:s}$). Since V_0 can be assumed to be finite in mixed regular-chaotic systems, we infer that the second-order process via the stronger coefficient V_1 will more dominantly contribute to the coupling between $|n\rangle$ and $|n+2r\rangle$ in the semiclassical limit $\hbar \to 0$.

A similar result is obtained from a comparison of the one-step process via V_k with the k-step process via V_1, where we again find that the latter more dominantly contributes to the coupling between $|n\rangle$ and $|n+kr\rangle$ in the limit $\hbar \to 0$. We therefore conclude that in mixed regular-chaotic systems the semiclassical tunneling process is adequately described by the lowest non-vanishing term of the sum over the V_k contributions, which in general is given by $V_1\cos(r\vartheta+\phi_1)$[4]. Neglecting all higher Fourier components V_k with $k>1$ and making the quadratic approximation of H_0 around $I=I_{r:s}$, we finally obtain an effective pendulum-like Hamiltonian

$$H_{\rm res}(I,\vartheta) \simeq \frac{(I-I_{r:s})^2}{2m_{r:s}} + 2V_{r:s}\cos(r\vartheta+\phi_1) \tag{8.24}$$

with $V_{r:s} \equiv V_1$ [31].

This simple form of the effective Hamiltonian allows us to determine the parameters $I_{r:s}$, $m_{r:s}$ and $V_{r:s}$ from the Poincaré map of the classical dynamics, without explicitly using the transformation to the action-angle variables of H_0. To this end, we numerically calculate the monodromy matrix $M_{r:s} \equiv \partial(p_f,q_f)/\partial(p_i,q_i)$ of a stable periodic point of the resonance (which involves r iterations of the stroboscopic map) as well as the phase space areas $S^+_{r:s}$ and $S^-_{r:s}$ that are enclosed by the outer and inner separatrices of the resonance, respectively (see also Fig. 8.3). Using the fact that the trace of $M_{r:s}$ as well as the phase space areas $S^\pm_{r:s}$ remain invariant under the canonical transformation to (I,ϑ), we infer

$$I_{r:s} = \frac{1}{4\pi}(S^+_{r:s}+S^-_{r:s})\,, \tag{8.25}$$

$$\sqrt{2m_{r:s}V_{r:s}} = \frac{1}{16}(S^+_{r:s}-S^-_{r:s})\,, \tag{8.26}$$

$$\sqrt{\frac{2V_{r:s}}{m_{r:s}}} = \frac{1}{r^2\tau}\arccos(\mathrm{tr}\,M_{r:s}/2) \tag{8.27}$$

[4]Exceptions from this general rule typically arise in the presence of discrete symmetries that, e.g., forbid the formation of resonance chains with an odd number of sub-islands and therefore lead to $V_1=0$ for an r:s resonance with an odd r.

from the integration of the dynamics generated by $H_{\rm res}$ [40]. Eqs. (8.25)-(8.27) make it possible to derive the final expressions for the tunneling rates directly from the dynamics of $H(t)$, without explicitly having to construct the integrable approximation H_0 and making the Fourier analysis of $V(p,q,t) = H(p,q,t) - H_0(p,q)$. As this construction of the integrable approximation may turn out to be highly non-trivial in the mixed regime, avoiding this step is actually an essential ingredient to make the approach we are following practical. We note though that improving the quadratic approximation (8.24) for H_0 is sometimes necessary, but this does not present any fundamental difficulty.

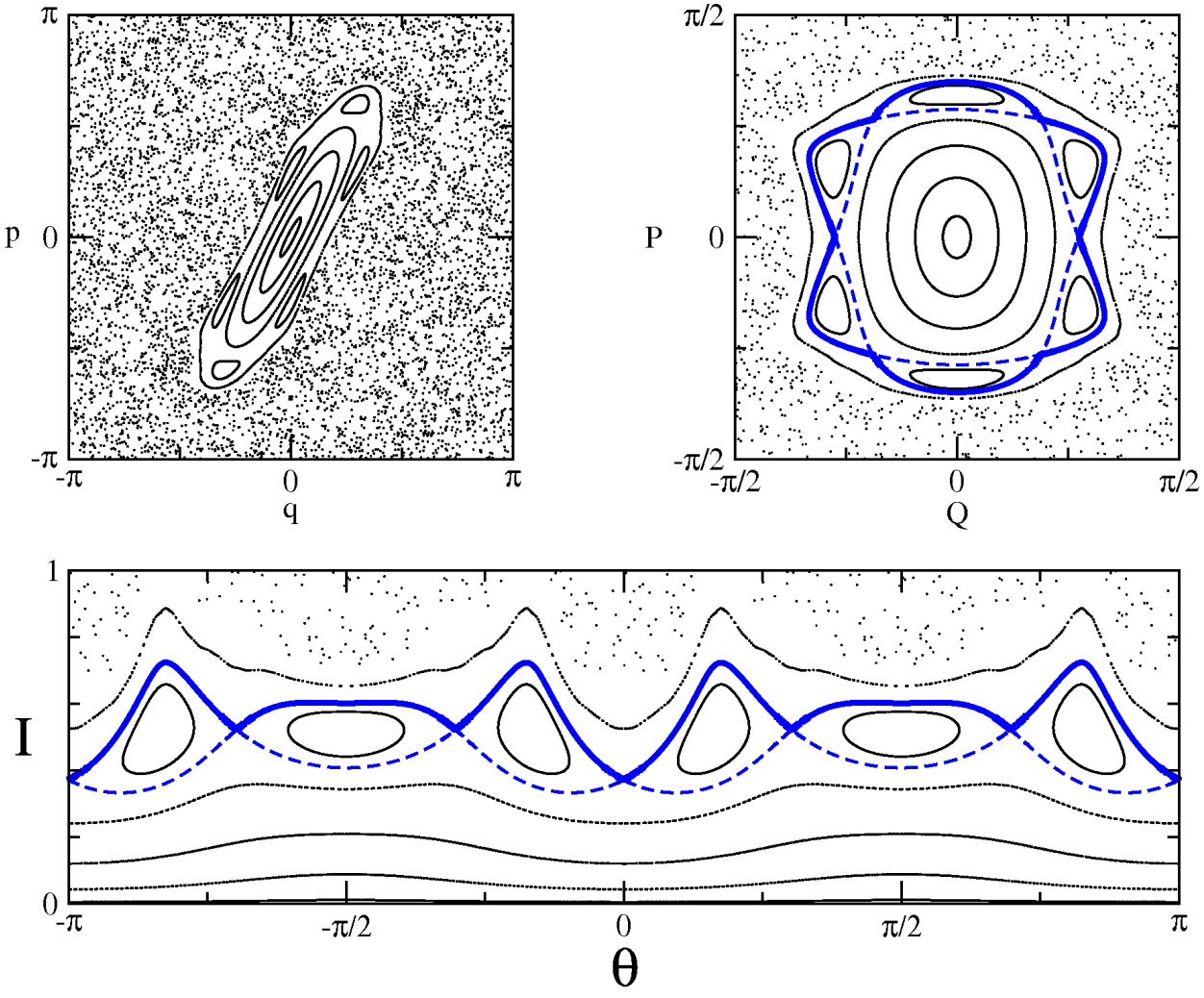

Figure 8.3: Classical phase space of the kicked rotor Hamiltonian at $K = 3.5$ showing a regular island with an embedded 6:2 resonance. The phase space is plotted in the original (p,q) coordinates (upper left panel), in approximate normal-form coordinates (P,Q) defined by Eqs. (8.28) and (8.29) (upper right panel), and in approximate action-angle variables (I,ϑ) (lower panel). The thick solid and dashed lines represent the "outer" and "inner" separatrix of the resonance, respectively.

8.2.3 Action dependence of the coupling coefficients

Up to now, and in our previous publications [27, 28, 31, 32, 33], we completely neglected the action dependence of the coupling coefficients $V_k(I)$. This approximation should be justified in the semiclassical limit of extremely small $\hbar$, where resonance-assisted tunneling generally involves multiple coupling processes [28] and transitions across individual resonance chains are therefore expected to take place in their immediate vicinity in action space. For finite $\hbar$, however, the replacement $V_k(I) \mapsto V_k(I_{r:s})$, permitting the direct quantization in action-angle space, is, in general, not sufficient to obtain an accurate reproduction of the quantum tunneling rates. We show now how this can be improved.

To this end, we make the general assumption that the classical Hamiltonian $H(p, q, t)$ of our system is analytic in p and q in the vicinity of the regular islands under consideration. It is then possible to define an analytical canonical transformation from (p, q) to Birkhoff-Gustavson normal-form coordinates (P, Q) [41, 42] that satisfy

$$P = -\sqrt{2I}\sin\theta\,, \tag{8.28}$$

$$Q = \sqrt{2I}\cos\theta \tag{8.29}$$

and that can be represented in power series in p and q. The "unperturbed" integrable Hamiltonian H_0 therefore depends only on $I = (P^2 + Q^2)/2$.

Writing

$$e^{\pm il\theta} = \left(\frac{Q \mp iP}{\sqrt{2I}}\right)^l \tag{8.30}$$

for positive l, we obtain, from Eq. (8.12), the series

$$V(I, \theta, t) = \sum_{m=-\infty}^{\infty} \left\{ V_{0,m}(I) + \sum_{l=1}^{\infty} \frac{1}{\sqrt{2I}^l} \left[V_{l,m}(I)(Q - iP)^l + V_{-l,m}(I)(Q + iP)^l \right] \right\} e^{im\omega t} \tag{8.31}$$

for the perturbation. Using the fact that $V(I, \theta, t)$ is analytic in P and Q, we infer that $V_{l,m}(I)$ must scale at least as $I^{l/2}$. By virtue of (8.14), this implies the scaling $V_k(I) \propto I^{rk/2}$ for the Fourier coefficients of the time-independent perturbation term that is associated with the r:s resonance. Making the ansatz $V_k(I) \equiv I^{rk/2}\tilde{v}_k$ (and neglecting the residual action dependence of $\tilde{v}_k$), we rewrite Eq. (8.13) as[5]

$$\mathcal{V}(I, \vartheta) = V_{0,0}(I) + \sum_{k=1}^{\infty} \frac{\tilde{v}_k}{2^{kr/2}} \left[(Q - iP)^{kr} e^{i\phi_k} + (Q + iP)^{kr} e^{-i\phi_k} \right] . \tag{8.32}$$

Each term in the sum is given by the well-known Birkhoff normal form generically describing a $r \geq 3$ resonance when the bifurcation of the stable periodic orbit is controlled by one single parameter (see, e.g., Eq. (4.70) in Chapter 4 of Ref. [43] or Eqs. (3.3.17) and (3.3.18) in Ref. [44] for another simple derivation of the action dependence of $V_k(I)$). The term $V_{0,0}(I)$ is neglected in the following as it does not lead to any coupling between different unperturbed eigenstates in the quantum system.

[5] This involves, strictly speaking, another canonical transformation of P and Q to the frame that co-rotates with the resonance.

One comment is in order here. The small parameter in the adiabatic approximation (8.10) is the difference $(I–I_{r:s})$, while in the derivation of Eq. (8.32) we have neglected higher powers of I and thus assumed the action I itself to be small (strictly speaking we should work near one bifurcation only). We thus mix a development near the resonant torus with one near the center of the island. This may eventually become problematic if (i) the resonance chain is located far away from the center of the island, in which case the associated coupling strength may contain a nonnegligible relative error when being computed via the assumption $V_k(I) \equiv I^{rk/2}\tilde{v}_k$ with constant $\tilde{v}_k$, and if (ii) that coupling strength happens to appear rather often in the main perturbative chain that connects the quasimodes of the island to the chaotic sea, which generally would be the case for low-order resonances with relatively small r.[6] Otherwise, we expect that this inconsistency in the definition of the regimes of validity of our perturbative approach does not lead to a significant impact on the numerical values of the semiclassical tunneling rates, which indeed seems to be confirmed by numerical evidence to be discussed below.

This being said, the quantization of the resulting classical Hamiltonian can now be carried out in terms of the "harmonic oscillator" variables P and Q and amounts to introducing the standard ladder operators $\hat{a}$ and $\hat{a}^\dagger$ according to

$$\hat{a} = \frac{1}{\sqrt{2\hbar}}(\hat{Q} + i\hat{P}) , \tag{8.33}$$

$$\hat{a}^\dagger = \frac{1}{\sqrt{2\hbar}}(\hat{Q} - i\hat{P}) . \tag{8.34}$$

This yields the quantum Hamiltonian

$$\hat{H}_{\rm res} = H_0(\hat{I}) - \Omega_{r:s}\hat{I} + \sum_{k=1}^{\infty} \tilde{v}_k \hbar^{kr/2} \left[\hat{a}^{kr} e^{-i\phi_k} + (\hat{a}^\dagger)^{kr} e^{i\phi_k}\right] \tag{8.35}$$

with $\hat{I} \equiv \hbar(\hat{a}^\dagger\hat{a}+1/2)$. As for Eq. (8.16), perturbative couplings are introduced only between unperturbed eigenstates $|n\rangle$ and $|n'\rangle$ that exhibit the selection rule $|n'-n| = kr$ with integer k. The associated coupling matrix elements are, however, different from Eq. (8.18) and read

$$\begin{aligned} \langle n+kr|\hat{H}_{\rm res}|n\rangle &= \tilde{v}_k \sqrt{\hbar}^{kr} e^{i\phi_k} \sqrt{\frac{(n+kr)!}{n!}} \\ &= V_k(I_{r:s}) e^{i\phi_k} \left(\frac{\hbar}{I_{r:s}}\right)^{kr/2} \sqrt{\frac{(n+kr)!}{n!}} \end{aligned} \tag{8.36}$$

for strictly positive k. Close the resonance, i.e. more formally taking the semiclassical limit $n \to \infty$ keeping k and $\delta = (I_{r:s}/\hbar - n)$ fixed, and making use of the Stirling formula $n! \simeq \sqrt{2\pi n}(n/e)^n$, Eq. (8.36) reduces to $V_k(I_{r:s})e^{i\phi_k}$. The difference becomes, on the other hand, particularly pronounced if the r:s resonance is, in phase space, rather asymmetrically located in between the invariant tori that correspond to the states $|n\rangle$ and $|n+kr\rangle$ — i.e., if $I_{r:s}$ is rather close to I_n or to I_{n+kr}. In that case, Eq. (8.18) may, respectively, strongly over- or underestimate the coupling strength between these states.

[6] Corrections to the form (8.32) should also arise in the presence of prominent *secondary* resonances, which occur when primary resonances start to overlap and create chains of sub-islands nested inside the primary island chains.

8.2.4 Multi-resonance processes

Up to this point, we considered the couplings between quasi-modes generated by a given resonance. In general, however, several of them may play a role for the coupling to the chaotic sea, giving rise to multi-resonance transitions across subsequent resonance chains in phase space [27, 28]. As was argued in the context of near-integrable systems [28], such multi-resonance processes are indeed expected to dominate over couplings involving only one single resonance in the deep semiclassical limit $\hbar \to 0$.

The description of the coupling process across several consecutive resonances requires a generalization of Eq. (8.19) describing the modified eigenstate due to resonance-induced admixtures. We restrict ourselves, for this purpose, to including only the first-order matrix elements $\langle n+r|\hat{H}_{\rm res}^{(r:s)}|n\rangle$ for each resonance [i.e., only the matrix elements with $k=1$ in Eq. (8.36)]. For the sake of clarity, we furthermore consider the particular case of coupling processes that start in the lowest locally quantized eigenmode with node number $n=0$ (the generalization to initial $n \neq 0$ being straightforward). The prescription we use is to consider that, although the approximation (8.15) is valid for only one resonance at a time, it is possible to sum the contributions obtained from different resonances. Considering a sequence of consecutive r:s, r':s', r'':s'' ... resonances, we obtain in this way

$$\begin{aligned}
|\psi_0\rangle \;=\; & |0\rangle + \sum_{k>0}\left(\prod_{l=1}^{k}\frac{\langle lr|\hat{H}_{\rm res}^{(r:s)}|(l-1)r\rangle}{E_0-E_{lr}+ls\hbar\omega}\right)\times \\
\times\; & \left\{|kr\rangle + \sum_{k'>0}\left(\prod_{l'=1}^{k'}\frac{\langle kr+l'r'|\hat{H}_{\rm res}^{(r':s')}|kr+(l'-1)r'\rangle}{E_0-E_{kr+l'r'}+(ks+l's')\hbar\omega}\right)\times\right. \\
& \times\left[|kr+k'r'\rangle + \sum_{k''>0}\left(\prod_{l''=1}^{k''}\frac{\langle kr+k'r'+l''r''|\hat{H}_{\rm res}^{(r'':s'')}|kr+k'r'+(l''-1)r''\rangle}{E_0-E_{kr+k'r'+l''r''}+(ks+l's'+l''s'')\hbar\omega}\right)\times\right. \\
& \left.\left.\times\left(|kr+k'r'+k''r''\rangle + \sum_{k'''>0}\ldots\right)\right]\right\}
\end{aligned} \tag{8.37}$$

for the modified "ground state" within the island. Given an excited quasi-mode n far from the interior of the island, the overlap $\langle n|\psi_0\rangle$ obtained from Eq. (8.37) will in most cases be exponentially dominated by one or a few contributions. There is no systematic way to identify them a priori, although some guiding principle can be used in this respect [28].

Quite naturally, for instance, low-order resonances, with comparatively small r and s, will, in general, give larger contribution than high-order resonances with comparable winding numbers s/r but larger r and s, due to the strong differences in the sizes of the mean coupling matrix elements $V_{r:s}$ [see, e.g., Eq. (8.22)]. In the same way, sequences of couplings involving small denominators, i.e. energy differences like Eq. (8.21) that are close to zero, and thus intermediate steps symmetrically located on each side of a resonance, will tend to give larger contributions. In the small $\hbar$ limit this will tend to favor multi-resonance processes. Conversely, for intermediate values of $\hbar$ (in terms of the area of the regular region) the main contributions can be obtained from the lowest-order resonances. With few exceptions — especially concerning low-order resonances that are located close to the center of the island, thereby leading to relatively large energy denominators and small admixtures — this rule is generally observed for the semiclassical calculation of the eigenphase splittings we shall

consider in section 8.4.

8.3 The combination with chaos-assisted tunneling

We now discuss the implication of such nonlinear resonances on the tunneling process between the two symmetry-related regular islands under consideration. In the quantum system, these islands support (for not too large values of $\hbar$) locally quantized eigenstates or "quasimodes" with different node numbers n, which, due to the symmetry, have the same eigenvalues in both islands. In our case of a periodically driven system, these eigenvalues can be the eigenphases φ_n of the unitary time evolution (Floquet) operator $\hat{U}$ over one period τ of the driving, or, alternatively, the quasienergies E_n such that $\varphi_n = -E_n\tau/\hbar$ (modulo 2π).

The presence of a small (tunneling-induced) coupling between the islands lifts the degeneracy of the eigenvalues and yields the symmetric and antisymmetric linear combination of the quasimodes in the two islands as "true" eigenstates of the system. A nonvanishing splitting $\Delta\varphi_n \equiv |\varphi_n^+ - \varphi_n^-|$ consequently arises between the eigenphases $\varphi_n^\pm$ of the symmetric and the antisymmetric state, which is related to the splitting $\Delta E_n \equiv |E_n^+ - E_n^-|$ of the quasi-energies $E_n^\pm$ through $\Delta\varphi_n = \tau\Delta E_n/\hbar$.

8.3.1 Resonance-assisted tunneling in near-integrable systems

We start by considering a system in the nearly integrable regime. In that case, we can assume the presence of a (global) integrable Hamiltonian $H_0(p,q)$ that describes the dynamics in the entire phase space to a very good approximation[7]. The energy splittings for the corresponding quantum Hamiltonian $\hat{H}_0 \equiv H_0(\hat{p},\hat{q})$ can be semiclassically calculated via an analytic continuation of the invariant tori to the complex domain [8]. This generally yields the splittings

$$\Delta E_n^{(0)} = \frac{\hbar\Omega_n}{\pi}\exp(-\sigma_n/\hbar) \tag{8.38}$$

(up to a numerical factor of order one) where Ω_n is the classical oscillation frequency associated with the nth quantized torus and σ_n denotes the imaginary part of the action integral along the complex path that joins the two symmetry-related tori.

The main effect of nonlinear resonances in the non-integrable system is, as was discussed in the previous subsections, to induce perturbative couplings between quasimodes of different excitation within the regular islands. For the nearly integrable systems this can already lead to a substantial enhancement of the splittings ΔE_n as compared to Eq. (8.38) [27, 28]. As can be derived within quantum perturbation theory, the presence of a prominent r:s resonance modifies the splitting of the local "ground state" in the island (i.e., the state with vanishing

[7]Formally, this Hamiltonian is not identical with the unperturbed approximation $H_0(I)$ introduced in section 8.2.1 as the definition of the latter is restricted to one well only. It is obvious, however, that $H_0(I)$ can be determined from $H_0(p,q)$, e.g. by means of the Lie transformation method [39].

node number $n = 0$) according to

$$\Delta\varphi_0 = \Delta\varphi_0^{(0)} + \sum_{k=1}^{k_c} |\mathcal{A}_{kr}^{(r:s)}|^2 \Delta\varphi_{kr}^{(0)} \tag{8.39}$$

(using $\Delta\varphi_n^{(0)} \gg \Delta\varphi_0^{(0)}$ for $n > 0$), where $\mathcal{A}_{kr}^{(r:s)} \equiv \langle kr|\psi_0\rangle$ denotes the admixture of the (kr)th excited unperturbed component $|kr\rangle$ to the perturbed ground state $|\psi_0\rangle$ according to Eq. (8.19) [possibly using Eq. (8.36) instead of (8.18)]. The maximal number k_c of coupled states is provided by the finite size of the island according to

$$k_c = \left[\frac{1}{r}\left(\frac{\text{area of the island}}{2\pi\hbar} - \frac{1}{2}\right)\right] \tag{8.40}$$

where the bracket stands for the integer part. The rapid decrease of the amplitudes $\mathcal{A}_{kr}^{(r:s)}$ with k is compensated by an exponential increase of the unperturbed splittings $\Delta\varphi_{kr}^{(0)}$, arising from the fact that the tunnel action σ_n in Eq. (8.38) generally decreases with increasing n. The maximal contribution to the modified ground state splitting is generally provided by the state $|kr\rangle$ for which $I_{kr} + I_0 \simeq 2I_{r:s}$ — i.e., which in phase space is most closely located to the torus that lies symmetrically on the opposite side of the resonance chain. This contribution is particularly enhanced by a small energy denominator [see Eq. (8.21)] and typically dominates the sum in Eq. (8.39).

As one goes further in the semiclassical $\hbar \to 0$ limit, a multi-resonance process is usually the dominant one. Neglecting interference terms between different coupling pathways that connect the ground state with a given excited mode $|n\rangle$ (which is justified due to the fact that the amplitudes associated with those coupling pathways are, in general, much different from each other in size), we obtain from Eq. (8.37) an expression of the form

$$\Delta\varphi_0 = \Delta\varphi_0^{(0)} + \sum_k |\mathcal{A}_{0,kr}^{(r:s)}|^2 \Delta\varphi_{kr}^{(0)} + \sum_k \sum_{k'} |\mathcal{A}_{0,kr}^{(r:s)}|^2 |\mathcal{A}_{kr,kr+k'r'}^{(r':s')}|^2 \Delta\varphi_{kr+k'r'}^{(0)} + \ldots \tag{8.41}$$

with the coupling amplitudes

$$\mathcal{A}_{0,kr}^{(r:s)} = \prod_{l=1}^{k} \frac{\langle lr|\hat{H}_{\text{res}}^{(r:s)}|(l-1)r\rangle}{E_0 - E_{lr} + ls\hbar\omega} \tag{8.42}$$

$$\mathcal{A}_{kr,kr+k'r'}^{(r':s')} = \prod_{l'=1}^{k'} \frac{\langle kr + l'r'|\hat{H}_{\text{res}}^{(r':s')}|kr + (l'-1)r'\rangle}{E_0 - E_{kr+l'r'} + (ks + l's')\hbar\omega} \tag{8.43}$$

$$\mathcal{A}_{kr+k'r',kr+k'r'+k''r''}^{(r'':s'')} = \ldots$$

for the eigenphase splitting.

8.3.2 Coupling with the chaotic sea

Turning now to the mixed regular-chaotic case, the integrable Hamiltonian $H_0(I)$ provides a good approximation only near the center of the regular island under consideration, and

invariant tori exist only up to a maximum action variable I_c corresponding to the outermost boundary of the regular island in phase space. Beyond this outermost invariant torus, multiple overlapping resonances provide various couplings and pathways such that unperturbed states in this regime can be assumed to be strongly connected to each other. Under such circumstances, it is natural to divide the Hilbert space into two parts, integrable and chaotic, associated respectively with the phase space regions within and outside the regular island.

For each symmetry class $\pm$ of the problem, let us introduce an effective Hamiltonian $\hat{H}^{\pm}_{\rm eff}$ modeling the tunneling process. Let us furthermore denote $\hat{P}_{\rm reg}$ and $\hat{P}_{\rm ch}$ the (orthogonal) projectors onto the regular and chaotic Hilbert spaces. The diagonal blocks $\hat{H}^{\pm}_{\rm reg} \equiv \hat{P}_{\rm reg}\hat{H}^{\pm}_{\rm eff}\hat{P}_{\rm reg}$ and $H^{\pm}_{\rm ch} \equiv \hat{P}_{\rm ch}\hat{H}^{\pm}_{\rm eff}\hat{P}_{\rm ch}$ receive a natural interpretation: within $\hat{H}^{\pm}_{\rm reg}$, on the one hand, the dynamics is exactly the same as in the nearly integrable regime above; $\hat{H}^{\pm}_{\rm ch}$, on the other hand, is best modeled in a statistical manner by the introduction of random matrix ensembles. The only remaining delicate point is thus to connect the two, namely to model the off-diagonal block $\hat{P}_{\rm reg}\hat{H}^{\pm}_{\rm eff}\hat{P}_{\rm ch}$. We stress that there is not yet a real consensus on the best way how to do this, although various approaches give good quantitative accuracy.

To state more clearly the problem, let us consider a regular state $|\bar{n}\rangle$ with quasi-energy $E^0_{\bar{n}}$ close to the regular-chaos boundary. (Note that "close" here means that no resonance within the island can connect $|\bar{n}\rangle$ to a state $|n'\rangle$ within the island with $n' > \bar{n}$. This notion of "closeness" to the boundary is therefore $\hbar$-dependent.) The resonance assisted mechanism will connect any quasi-mode deep inside the island to such a state at the edge of the island. But to complete the description of the chaos-assisted tunneling process it is necessary to compute the variance $v^2_{\bar{n}}$ of the random matrix elements $v_{\bar{n}i}$ between $|\bar{n}\rangle$ and the eigenstates $|\psi^c_i\rangle$ of $\hat{H}^{\pm}_{\rm ch}$ (the variance is independent of i if $\hat{H}^{\pm}_{\rm ch}$ is modeled by the Gaussian orthogonal or unitary ensemble).

One possible approach to compute this quantity is the fictitious integrable system approach that was proposed by Bäcker et al. [22]. This method relies on the fact that, for the effective Hamiltonian $\hat{H}_{\rm eff}$, the "direct" transition rate from a regular state $|n\rangle$ to the chaotic region is given using Fermi's golden rule by

$$\Gamma^d_{n\to{\rm chaos}} = \frac{2\pi}{\hbar}\frac{v_n^2}{\Delta_{\rm ch}}\ , \tag{8.44}$$

(see e.g. section 5.2.2 of Ref. [11] for a discussion in the context of random matrix theory) where $\Delta_{\rm ch}$ denotes the mean spacing between eigenenergies within the chaotic block. As a consequence, one obtains in first order in $\tau v_n^2/\hbar\Delta_{\rm ch}$,

$$||\hat{P}_{\rm ch}\hat{U}|n\rangle||^2 = \tau\Gamma^d_{n\to{\rm chaos}} = \frac{2\pi\tau}{\hbar}\frac{v_n^2}{\Delta_{\rm ch}} \tag{8.45}$$

(see also the contribution of Bäcker, Ketzmerick, and Löck in this book). If one can explicitly construct a good integrable approximation $H_{\rm reg} \equiv H_0(p,q)$ of the time-dependent dynamics (see Sec. 8.2.1), this allows one, by quantum or semiclassical diagonalization, to determine the unperturbed eigenstates $|n\rangle$ within the regular island, and to construct the projectors $\hat{P}_{\rm reg}$ and $\hat{P}_{\rm ch}$ The "direct" regular-to-chaotic tunneling matrix elements of the nth quantized state within the island is then evaluated by a simple application of the quantum time evolution operator $\hat{U}$ over one period of the driving.

This approach can be qualified as "semi-numerical", as it requires to numerically perform the quantum evolution for one period of the map (although this can be done by analytical and semiclassical techniques in some cases [23], see also the contribution of Bäcker et al. in this book). It strongly relies on the quality of the integrable approximation $\hat{H}_{\rm reg}$ of the Hamiltonian. If the latter was really diagonal (which, as a matter of principle, cannot be achieved by means of classical perturbation theory, due to the appearance of nonlinear resonances), Eq. (8.45) would represent an exact result (apart from the first-order approximation in $\tau v_n^2/\hbar\Delta_{\rm ch}$ which should not be a limitation in the tunneling regime). And indeed very good agreement between this prediction and numerically computed tunneling rates was found for quantum maps that were designed such as to yield a "clean" mixed regular-chaotic phase space, containing a regular island and a chaotic region which both do not exhibit appreciable substructures [22], as well as for the mushroom billiard [23]. In more generic situations, where nonlinear resonances are manifested within the regular island, this approach yields reliable predictions for the direct tunneling of regular states at the regular-chaos border, and its combination with the resonance assisted mechanism described in the previous sections leads to good quantitative predictions for the tunneling rates for the states deep in the regular island [35]. We shall illustrate this on the example of the kicked rotor system in section 8.4.

8.3.3 Integrable semiclassical models for the regular-to-chaotic coupling

For now, however, we shall discuss other possible approaches of purely semiclassical nature (i.e. not involving any numerical evolution nor diagonalization of the quantum system) to the calculation of the coupling parameter $v_{\bar{n}}$ for a regular state $|\bar{n}\rangle$ at the edge of the regular-chaos boundary.

One way to obtain an order of magnitude of $v_{\bar{n}}^2$ is to consider the decay of the quasimode inside the regular island. For this purpose, let us assume that an integrable approximation $H_0(I)$, valid up to a maximum action I_c corresponding to the chaos boundary, has been obtained. Within the Birkhoff-Gustavson normal-form coordinates (P,Q) given by Eqs. (8.28) and (8.29), H_0 appears as a function of the harmonic-oscillator Hamiltonian $(P^2+Q^2)/2$ and therefore has the same eigenstates

$$\langle Q|\ \bar{n}\rangle = \frac{1}{\sqrt{2^{\bar{n}}\bar{n}!}}\frac{1}{(\pi\hbar)^{1/4}}\exp\left(-Q^2/2\hbar\right)\mathcal{H}_{\bar{n}}(Q/\hbar^{1/2}) \tag{8.46}$$

$$\simeq \frac{1}{2\sqrt{2\pi|P_{\bar{n}}(Q)|}}\exp\left(-\int_{Q_1}^{Q}|P_{\bar{n}}(Q)|dQ\right) \qquad \text{for} \quad Q>Q_n\ , \tag{8.47}$$

where $\mathcal{H}_{\bar{n}}$ are the Hermite polynomials and $P_{\bar{n}}(Q)=\sqrt{2I_{\bar{n}}-Q^2}$. The last equation corresponds to the semiclassical asymptotics in the forbidden region on the right-hand side of the turning point $Q_1=\sqrt{2I_{\bar{n}}}$ with $I_{\bar{n}}=\hbar(\bar{n}+1/2)$. In Q representation, the regular island extends up to $Q_c=\sqrt{2I_c}$, at which point de state $|\bar{n}\rangle$ has decayed to $\psi_{\bar{n}}(Q_c)\simeq \frac{1}{2\sqrt{2\pi|P_{\bar{n}}(Q_c)|}}\exp\left(-S(I_{\bar{n}},I_c)\right)$, where

$$S(I_{\bar{n}},I_c)=\int_{Q_1}^{Q_c}|P_{\bar{n}}(Q)|dQ=\sqrt{I_c(I_c-I_{\bar{n}})}-I_n\ln\left((\sqrt{I_c-I_{\bar{n}}}+\sqrt{I_c})/\sqrt{I_{\bar{n}}}\right)\ . \tag{8.48}$$

This expression is suspiciously simple (as it depends only on $I_{\bar{n}}$ and I_c, and on no other property of the system), and should not be taken too seriously as it is.

Indeed, it should be borne in mind that $v_{\bar{n}}^2$ is related not so much to the value of the wavefunction at the regular-chaos boundary than to the transition rate $\Gamma^d_{n\to\text{chaos}}$ through Eq. (8.44), which we can equal to the current flux $J_{\bar{n}}$ through this boundary for the regular state $|\bar{n}\rangle$. Using $H_0(I)$ to compute this current leads to a zero result and it is therefore mandatory to use a better approximation of the non-integrable Hamiltonian H to obtain a meaningful answer. What complicates the evaluation of the transition rate from the edge of the regular to the chaotic domain is therefore that one needs to find an approximation describing both the regular and chaotic dynamics — unless one actually uses there the exact quantum dynamics as was done in Ref. [22]. Since the regular-chaos border is typically the place where approximation schemes tend to be difficult to control, this will rely on some assumption to be made for the chaotic regions, two possible choices of which we shall describe now.

One scenario that has been considered amounts in some way to model the regular to chaos transition in the way depicted in Fig. 8.4a: a kinetic-plus-potential Hamiltonian $p^2/2m+V(q)$ where the island itself correspond to a potential well and the edge of the regular region to the place where the potential decreases abruptly. The picture one has in mind in that case is that escaping from the edge of the regular island to the chaotic sea is akin to the standard textbook barrier tunneling [45]. Using Langer's connection formula [46] within that model, the semiclassical wavefunction for the quasi-mode $\bar{n}$ inside the potential well can be extended under the potential barrier and, beyond this, into the region where motion at energy $E^0_{\bar{n}}$ is again classically authorized. In the classically allowed region outside the well ($q > q'_r$) the semiclassical wavefunction can be written as

$$\psi_{\bar{n}}(q) \simeq \sqrt{\frac{\Omega_{\bar{n}}}{2\pi p_{\bar{n}}(q)}} \exp\left(\frac{i}{\hbar}\int_{q'_r}^{q} p_{\bar{n}}(q)dq + i\pi/4\right) \exp\left(-\frac{S_\text{t}}{\hbar}\right) \ , \tag{8.49}$$

with $\Omega_{\bar{n}}$ the angular frequency of the torus $E^0_{\bar{n}}$, $p_{\bar{n}}(q) = \sqrt{2m[E^0_{\bar{n}} - V(q)]}$, and

$$S_\text{t} = \int_{q_r}^{q'_r} |p_{\bar{n}}(q)|dq \tag{8.50}$$

the tunneling action[8]. The current of probability leaving the well is then given by

$$J_{\bar{n}} \equiv \frac{\hbar}{m}\,\text{Im}[\psi^*_{\bar{n}}\nabla\psi_{\bar{n}}] = \frac{\Omega_{\bar{n}}}{2\pi}\exp\left(-2\frac{S_\text{t}}{\hbar}\right) \ , \tag{8.51}$$

from which $v_{\bar{n}}^2$ is obtained through Eq. (8.44) (identifying $J_{\bar{n}}$ with $\Gamma^d_{\bar{n}\to\text{chaos}}$).

Although Eq. (8.51) is derived here for the particular case of a kinetic-plus-potential Hamiltonian, it applies more generally (up maybe to factors of order one) to any system with a phase space portrait that is similar to the one of Fig. 8.4b, where tori inside the island can be analytically continued in the complex plane to a manifold escaping to infinity.

[8]Strictly speaking, outgoing (Siegert) boundary conditions [47] need to be employed in Eq. (8.49) in order to properly describe the decay process from the well. Those outgoing boundary conditions involve, in addition, an exponential increase of the wavefunction's amplitude with increasing distance from the well, which is not taken into account in Eq. (8.49) assuming that the tunneling rate from the well is comparatively weak.

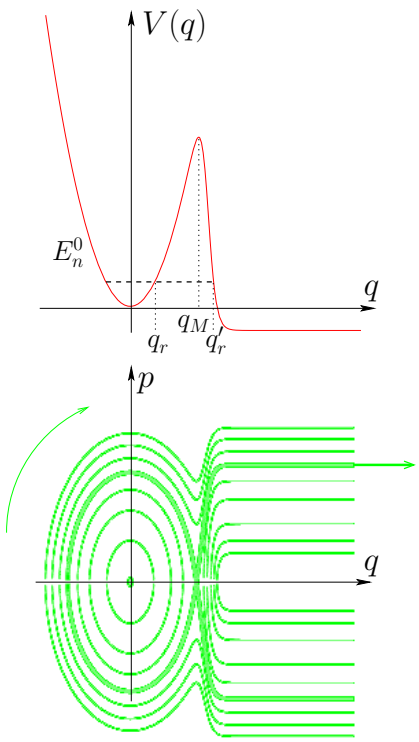

Figure 8.4: Modeling of the direct coupling between the edge of the regular region to the chaotic one by a potential barrier separating a potential well from an "open" region. (a) Sketch of the potential. (b) Corresponding phase space portrait.

In that case, Eq. (8.51) can be applied provided the tunneling action S_t is taken as the imaginary part of the action integral on a path joining the interior to the exterior of the island on this analytical continuation. As a last approximation, one may assume that the transition to the "open" part is extremely sharp once the separatrix is crossed. In the model of Fig. 8.4a, this amounts to assume a very rapid decrease of the potential, in which case one may replace q_r by q_M in the tunneling action Eq. (8.50). In an actual calculation of the direct tunneling rate for a regular state at the edge of the chaos boundary (which we can reliably describe only coming from the interior of the island) this amounts to consider in the same way that the action $S(I_{\bar{n}}, I_c)$ [Eq. (8.48)] provides a good approximation to S_t. Under this hypothesis, one obtains for the coupling to the chaotic Hilbert space the prediction

$$v_{\bar{n}}^2 = \frac{\Delta_{\rm ch}\hbar\Omega_{\bar{n}}}{4\pi^2}\exp\left(-2\frac{S(I_{\bar{n}}, I_c)}{\hbar}\right) \tag{8.52}$$

(see [48] where this computation was proposed with the slightly different language of complex time trajectories).

This "potential-barrier" picture of the direct tunneling is in essence what is behind the approach of Podolskiy and Narimanov [19] (though their treatment of the problem is a bit more sophisticated). Its main virtue is that, beyond the quantized action $I_{\bar{n}} = \hbar(\bar{n} + 1/2)$, Eq. (8.52) relies only on simple characteristics of the integrable regions : its area $2\pi I_c$ and the frequency $\Omega_{\bar{n}}$ of the torus $I_{\bar{n}}$. One needs to keep in mind, however, that Eq. (8.52) implicitly

assumes that the direct tunneling mechanism corresponds in some sense to the phase portrait of Fig. 8.4b, which in general cannot be justified within any controlled approximation scheme.

8.3.4 Regular-to-chaotic coupling via a nonlinear resonance

Another possible, and presumably more realistic, approach to evaluate the direct coupling parameter $v_{\bar{n}}$ can be obtained assuming that the effective model (8.15) describes the vicinity of a resonance not only inside the regular region, but also within the chaotic sea in the near vicinity of the island. In this perspective, the model one has in mind for the chaotic region follows the spirit of Chirikov's overlapping criterion for the transition to chaos [49, 39]: resonances still provide the couplings between quasi-modes, but in the chaotic region these couplings become strong enough to completely mix the states. Near the regular-chaos edge, the transition between modes inside and outside the regular region is still dominated by one or several r:s resonances which might be within or possibly outside the regular island.

As an illustration, let us consider the simple case where a single nonlinear r:s resonance is responsible for all couplings, both within the island and from the island's edge to the chaotic region. Keeping in mind the discussion in Section 8.2.2 and in Ref. [28], we assume here that the couplings induced by the r:s resonance are dominantly described by the lowest non-vanishing Fourier component V_1 of the perturbation, i.e. by the matrix elements $V_{r:s}^{(n+r)} \equiv \langle n+r|\hat{H}_{\rm eff}|n\rangle$, and set the phase ϕ_1 to zero without loss of generality.

The structure of the effective Hamiltonian that describes the coupling of the ground state E_0 to the chaotic sea is, in that case, given by

$$H_{\rm eff}^{\pm} = \begin{pmatrix} \tilde{E}_0 & V_{r:s}^{(r)} & & & \\ V_{r:s}^{(r)} & \ddots & \ddots & & \\ & \ddots & \tilde{E}_{k_c r} & V_{r:s}^{[(k_c+1)r]} & \\ & & V_{r:s}^{[(k_c+1)r]} & \boxed{\text{chaos}^{\pm}} & \end{pmatrix}, \tag{8.53}$$

where $\tilde{E}_{kr} \equiv E_{kr} - \Omega_{r:s} I_{kr}$ are the eigenenergies of the unperturbed Hamiltonian $\mathcal{H}_0$ in the co-rotating frame, and the chaotic part (the square in the lower right corner) consists of a full sub-block with equally strong couplings between all basis states with actions beyond the outermost invariant torus of the islands. In this example the last state within the island connected to the ground state is the quasi-mode $\bar{n} = k_c r$ and $v_{\bar{n}}^2 = (V_{r:s}^{[(k_c+1)r]})^2/N_{\rm ch}$, with $N_{\rm ch}$ the number of states with a given parity in the chaotic Hilbert space. In a more general situation, many resonances may, as in Eq. (8.37), be involved in connecting the ground stated to some $|\bar{n}\rangle$ at the edge of the island, but we would still write the variance $v_{\bar{n}}^2$ of the matrix elements providing the last coupling to the chaotic region as the ratio $(V_{r:s}^{[(k_c+1)r]})^2/N_{\rm ch}$ for some r:s resonance near the regular-chaos edge.

We stress here that it is necessary in this approach to have an explicit access to the number of states $N_{\rm ch}$ in the chaotic Hilbert space. This is obtained quite trivially for quantum maps, such as the kicked rotor we shall consider in section 8.4, when $\hbar = 2\pi/N$ with integer N. In that case N is the total number of states in the full Hilbert space and $N_{\rm ch}/N$ represents the relative area of the chaotic region in phase space. For a two dimensional conservative Hamiltonian, on the other hand, N and thus $N_{\rm ch}$ are related to the Thouless energy (see e.g. the section 2.1.4 of [50]), but this provides only an energy scale rather than a precise number, and a more detailed discussion is required to be quantitative. For the sake of clarity, we shall in the following limit our discussion to the simpler case that N is known.

8.3.5 Theory of chaos-assisted tunneling

Let us consider now the effect of the chaotic block on the tunneling process. Eliminating intermediate states within the regular island leads for the effective Hamiltonian a matrix of the form

$$H_{\rm eff}^{\pm} = \begin{pmatrix} E_0 & V_{\rm eff} & 0 & \cdots & 0 \\ V_{\rm eff} & H_{11}^{\pm} & \cdots & \cdots & H_{1N_{\rm ch}}^{\pm} \\ 0 & \vdots & & & \vdots \\ \vdots & \vdots & & & \vdots \\ 0 & H_{N_{\rm ch}1}^{\pm} & \cdots & \cdots & H_{N_{\rm ch}N_{\rm ch}}^{\pm} \end{pmatrix} . \tag{8.54}$$

for each symmetry class. In the simplest case Eq. (8.53) where a single r:s resonance needs to be considered, the effective coupling matrix element between the ground state and the chaos block ($H_{ij}^{\pm}$) is given by

$$V_{\rm eff} = V_{r:s}^{[(k_c+1)r]} \prod_{k=1}^{k_c} \frac{V_{r:s}^{(kr)}}{E_0 - E_{kr} + ks\hbar\omega} \tag{8.55}$$

where E_n are the unperturbed energies (8.20) of $H_{\rm eff}$ and $|k_c r\rangle$ represents the highest unperturbed state that is connected by the r:s resonance to the ground state and located within the island (i.e., $I_{k_c r} < I_c < I_{(k_c+1)r}$). More generally, $V_{\rm eff}$ can be expressed in terms of the couplings associated with the various resonances that contribute to the transitions within the island and at the regular-chaos edge. The form of this expression (8.55) already provides an explanation for the appearance of plateau-like structures in the tunneling rates. Indeed, decreasing $\hbar$ leads to discontinous increments of the maximal number k_c of couplings through Eq. (8.40) and hence to step-like reductions of the effective matrix element $V_{\rm eff}$, while in between such steps $V_{\rm eff}$ varies smoothly through the action dependence of the coupling matrix elements $V_{r:s}^{(kr)}$, provided accidential near-degeneracies in the energy denominators do not occur.

In the simplest possible approximation, which follows the lines of Refs. [12, 17], we neglect the effect of partial barriers in the chaotic part of the phase space [11] and assume that the chaos block ($H_{ij}^{\pm}$) is adequately modeled by a random Hermitian matrix from the Gaussian orthogonal ensemble (GOE). After a pre-diagonalization of ($H_{ij}^{\pm}$), yielding the eigenstates $\phi_j^{\pm}$ and eigenenergies $\mathcal{E}_j^{\pm}$, we can perturbatively express the shifts of the symmetric and

antisymmetric ground state energies by

$$E_0^{\pm} = E_0 + \sum_{j=1}^{N_{\rm ch}} \frac{|v^j_{{\rm eff}\pm}|^2}{E_0 - \mathcal{E}_j^{\pm}} \,, \tag{8.56}$$

with $v^j_{{\rm eff}\pm} \equiv V_{\rm eff}\langle kr|\phi_j^{\pm}\rangle$ Performing the random matrix average for the eigenvectors, we obtain that $\langle\langle|\langle kr|\phi_j^{\pm}\rangle|^2\rangle\rangle \simeq 1/N_{\rm ch}$ for all $j = 1 \ldots N_{\rm ch}$, which simply expresses the fact that none of the basis states is distinguished within the chaotic block ($H_{ij}^{\pm}$). As a consequence, the variance of the $v^j_{{\rm eff}\pm}$'s is independent of j and equal to $v^2_{\rm eff} = V^2_{\rm eff}/N_{\rm ch}$.

As was shown in Ref. [17], the random matrix average over the eigenvalues $\mathcal{E}_j^{\pm}$ gives rise to a Cauchy distribution for the shifts of the ground state energies, and consequently also for the splittings

$$\Delta E_0 = |E_0^+ - E_0^-| \tag{8.57}$$

between the symmetric and the antisymmetric ground state energy. For the latter, we specifically obtain the probability distribution

$$P(\Delta E_0) = \frac{2}{\pi} \frac{\overline{\Delta E_0}}{(\Delta E_0)^2 + (\overline{\Delta E_0})^2} \tag{8.58}$$

with

$$\overline{\Delta E_0} = \frac{2\pi v^2_{\rm eff}}{\Delta_{\rm ch}} \tag{8.59}$$

where $\Delta_{\rm ch}$ denotes the mean level spacing in the chaos at energy E_0. This distribution is, strictly speaking, valid only for $\Delta E_0 \ll v_{\rm eff}$ and exhibits a cutoff at $\Delta E_0 \sim 2v_{\rm eff}$, which ensures that the statistical expectation value $\langle \Delta E_0\rangle = \int_0^{\infty} xP(x)dx$ does not diverge.

Since tunneling rates and their parametric variations are typically studied on a logarithmic scale [i.e., $\log(\Delta E_0)$ rather than ΔE_0 is plotted vs. $1/\hbar$], the relevant quantity to be calculated from Eq. (8.58) and compared to quantum data is not the mean value $\langle \Delta E_0\rangle$, but rather the average of the logarithm of ΔE_0. We therefore define our "average" level splitting $\langle \Delta E_0\rangle_g$ as the *geometric* mean of ΔE_0, i.e.

$$\langle \Delta E_0\rangle_g \equiv \exp\left[\langle \ln(\Delta E_0)\rangle\right] \tag{8.60}$$

and obtain as result the scale defined in Eq. (8.59),

$$\langle \Delta E_0\rangle_g = \overline{\Delta E_0}\,. \tag{8.61}$$

This expression further simplifies for our specific case of periodically driven systems, where the time evolution operator $\hat{U}$ is modeled by the dynamics under the effective Hamiltonian (8.54) over one period τ. In this case, the chaotic eigenphases $\mathcal{E}_j^{\pm}\tau/\hbar$ are uniformly distributed in the interval $[0, 2\pi[$. We therefore obtain

$$\Delta_{\rm ch} = \frac{2\pi\hbar}{N_{\rm ch}\tau} \tag{8.62}$$

for the mean level spacing near E_0. This yields

$$\langle \Delta\varphi_0 \rangle_g \equiv \frac{\tau}{\hbar} \langle \Delta E_0 \rangle_g = \left(\frac{\tau V_{\rm eff}}{\hbar} \right)^2 \tag{8.63}$$

for the geometric mean of the ground state's eigenphase splitting. Note that this final result does not depend on the number $N_{\rm ch}$ of chaotic states within the sub-block ($H_{ij}^{\pm}$); as long as this number is sufficiently large to justify the validity of the Cauchy distribution (8.58) (see Ref. [17]), the geometric mean of the eigenphase splitting is essentially given by the square of the effective coupling $V_{\rm eff}$ from the ground state to the chaos.

The distribution (8.58) also permits the calculation of the logarithmic variance of the eigenphase splitting: we obtain

$$\left\langle \left[\ln(\Delta\varphi_0) - \langle \ln(\Delta\varphi_0) \rangle \right]^2 \right\rangle = \frac{\pi^2}{4} \,. \tag{8.64}$$

This universal result predicts that the actual splittings may be enhanced or reduced compared to $\langle \Delta\varphi_0 \rangle_g$ by factors of the order of $\exp(\pi/2) \simeq 4.8$, independently of the values of $\hbar$ and external parameters. Indeed, as was discussed in Ref. [32], short-range fluctuations of the splittings, arising at small variations of $\hbar$, are well characterized by the standard deviation that is associated with Eq. (8.64).

It is interesting to note that the expression (8.63) for the (geometric) mean level spacing is quantitatively identical with the expression (8.45) for the mean escape rate from the regular island to the chaotic sea derived in Ref. [22] using Fermi's golden rule. This seems surprising as two different nonclassical processes, namely Rabi oscillations between equivalent islands and the decay from an island within an open system, underly these expressions. In one-dimensional single-barrier tunneling problems, these two processes would indeed give rise to substantially different rates; in Eq. (8.1), to be more precise, the imaginary action integral in the exponent would have to be multiplied by two in order to obtain the corresponding expression for the decay rate (and the overall prefactor in front of the exponential function should be divided by two, which is not important here). The situation is a bit different, however, in our case of dynamical tunneling in mixed regular-chaotic systems. In such systems, level splittings between two equivalent regular islands involve *two* identical dynamical tunneling processes between the islands and the chaotic sea (namely one process for each island), while the decay into the chaotic sea involves only *one* such process, with, however, the square of the corresponding (exponentially suppressed) coupling coefficient. This explains from our point of view the equivalence of the expressions (8.63) and (8.45).

We finally remark that the generalization of the expression for the mean splittings to multi-resonance processes is straightforward and amounts to replacing the product of admixtures in Eq. (8.55) by a product involving several resonances subsequently, in close analogy with Eq. (8.41). In fact, the multi-resonance expression (8.41) can be directly used in this context replacing the "direct" splittings $\Delta\varphi_n^{(0)}$ by $(V_{r_f:s_f}^{[(k_c+1)r_f]}\tau/\hbar)^2$ where the r_f:s_f resonance is the one that induces the final coupling step to the chaotic sea (provided $I_n < I_c < I_{n+r_f}$ holds for the corresponding action variables; otherwise we would set $\Delta\varphi_n^{(0)} = 0$). This expression represents the basic formula that is used in the semiclassical calculations of the splittings in the kicked rotor model, to be discussed below.

8.3.6 The role of partial barriers in the chaotic domain

In the previous section, we assumed a perfectly homogeneous structure of the Hamiltonian outside the outermost invariant torus, which allowed us to make a simple random-matrix ansatz for the chaotic block. This assumption hardly ever corresponds to reality. As was shown in Refs. [51, 11, 12] for the quartic oscillator, the chaotic part of the phase space is, in general, divided into several subregions which are weakly connected to each other through partial transport barriers for the classical flux (see, e.g., Fig. 8 in Ref. [12]) This substructure of the chaotic phase space (which is generally not visible in a Poincaré surface of section) is particularly pronounced in the immediate vicinity of a regular island, where a dense hierarchical sequence of partial barriers formed by broken invariant tori and island chains is accumulating [52, 53, 54].

In the corresponding quantum system, such partial barriers may play the role of "true" tunneling barriers in the same spirit as invariant classical tori. This will be the case if the phase space area ΔW that is exchanged across such a partial barrier within one classical iteration is much smaller than Planck's constant $2\pi\hbar$ [55], while in the opposite limit $\Delta W \gg 2\pi\hbar$ the classical partial barrier appears completely transparent in the quantum system[9]. Consequently, the "sticky" hierarchical region around a regular island acts, for not extremely small values of $\hbar$, as a dynamical tunneling area and thereby extends the effective "quantum" size of the island in phase space. As a matter of fact, this leads to the formation of localized states (also called "beach" states in the literature [13]) which are supported by this sticky phase space region in the surrounding of the regular island [56] (see Fig. 8.6b).

An immediate consequence of the presence of such partial barriers for resonance-assisted tunneling is the fact that the critical action variable I_c defining the number k_c of resonance-assisted steps within the island according to Eq. (8.55) should not be determined from the outermost invariant torus of the island, but rather from the outermost partial barrier that acts like an invariant torus in the quantum system. We find that this outermost quantum barrier is, for not extremely small values of $\hbar$, generally formed by the stable and unstable manifolds that emerge from the hyperbolic periodic points associated with a low-order nonlinear r:s resonance. These manifolds are constructed until their first intersection points in between two adjacent periodic points, and iterated $r-1$ times (or $r/2-1$ times in the case of period-doubling of the island chain due to discrete symmetries), such as to form a closed artificial boundary around the island in phase space[10] As shown in Fig. 8.5, one further iteration maps this boundary onto itself, except for a small piece that develops a loop-like deformation. The phase space area enclosed between the original and the iterated boundary precisely defines the classical flux ΔW exchanged across this boundary within one iteration of the map [52, 53].

The example in Fig. 8.5 shows a boundary that arises from the inner stable and unstable manifolds (i.e. the ones that would, in a near-integrable system, form the inner separatrix structure) emerging from the unstable periodic points of a 4:1 resonance (which otherwise is not visible in the Poincaré section) in the kicked rotor system. Judging from the size of the flux area ΔW, this boundary should represent the relevant quantum chaos border for the tunneling processes that are discussed in the following section. We clearly see that it

[9] More precisely, the authors of Ref. [55] claim that ΔW has to be compared with $\pi\hbar$ in order to find out whether or not a given partial barrier is transparent in the quantum system.

[10] This construction is also made in order to obtain the phase space areas $S^{\pm}_{r:s}$ that are enclosed by the outer and inner separatrix structures of an r:s resonance, and that are needed in order to compute the mean action variable $I_{r:s}$ and the coupling strength $V_{r:s}$ of the resonance according to Eqs. (8.26) and (8.27).

encloses a non-negligible part of the chaotic classical phase space, which includes a prominent 10:3 resonance that, consequently, needs to be taken into account for the coupling process between the regular island and the chaotic sea. Thereby, we naturally arrive at *multi-step* coupling processes across a sequence of several resonances, which would have to be computed for a reliable prediction of the tunneling rates in the semiclassical regime.

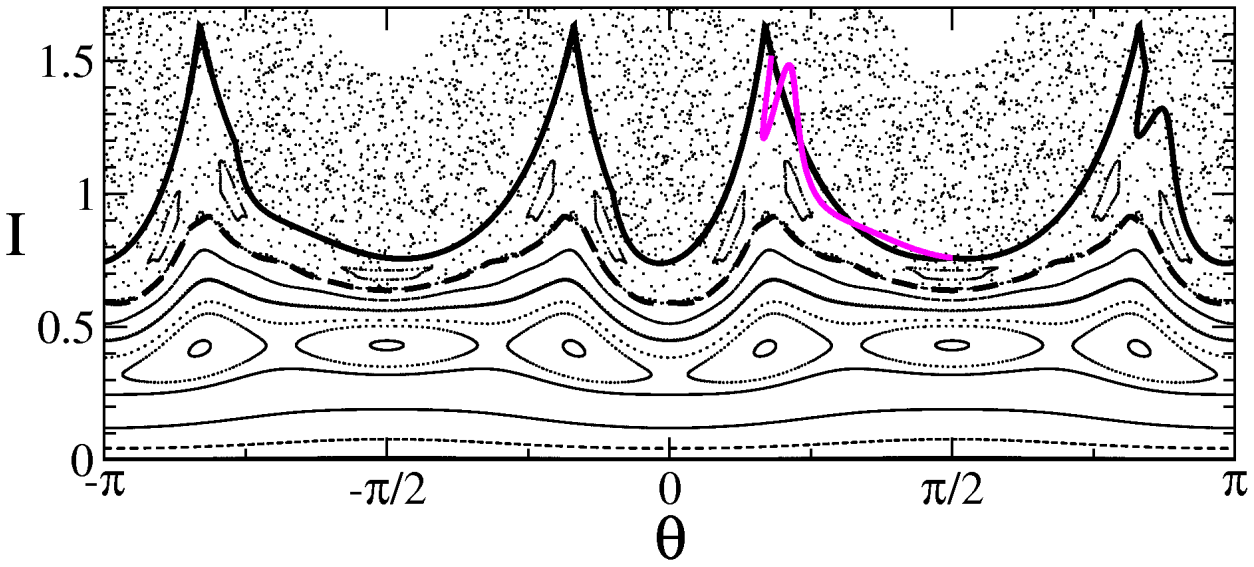

Figure 8.5: Classical phase space of the kicked rotor at $K = 3.4$ in approximate action-angle variables (I, θ). The thick solid line shows the location of the effective quantum boundary of the central island for the values of Planck's constant that are considered in Section 8.4. This effective boundary is constructed from segments of the stable and unstable manifolds that emerge from the hyperbolic periodic points of the 4:1 resonance at $\theta \simeq \pi/6$ and $5\pi/6$, respectively. Those segments were computed until the symmetry axis at $\theta = \pi/2$ and then iterated three times under the kicked rotor map, yielding the thick solid line. A further iteration of this boundary maps it onto itself, except for the piece between $\theta \simeq 0.15\pi$ and $\theta = 0.5\pi$ which is replaced by the lighter curve. The phase space area that is enclosed between the original (dark) and the iterated (light) boundary defines the classical flux that is exchanged across this boundary within one iteration of the map. The dashed line shows, in comparison, the actual classical chaos border defined by the outermost invariant torus of the island.

8.4 Application to the kicked rotor

8.4.1 Tunneling in the kicked rotor

To demonstrate the validity of our approach, we apply it to the "kicked rotor" model, which is described by the Hamiltonian

$$H(p, q, t) = p^2/2 - K \sum_{n=-\infty}^{\infty} \delta(t - n) \cos q \,. \tag{8.65}$$

The classical dynamics of this system is described by the "standard map" $(p,q) \mapsto (p',q')$ with

$$p' = p - K\sin q \tag{8.66}$$
$$q' = q + p' , \tag{8.67}$$

which generates the stroboscopic Poincaré section at times immediately before the kick. The phase space of the kicked rotor is 2π periodic in position q and momentum p, and exhibits, for not too large perturbation strengths $K < 4$, a region of bounded regular motion centered around $(p,q) = (0,0)$.

The quantum dynamics of the kicked rotor is described by the associated time evolution operator

$$\hat{U} = \exp\left(-\frac{i}{\hbar}\frac{\hat{p}^2}{2}\right)\exp\left(-\frac{i}{\hbar}K\cos\hat{q}\right) \tag{8.68}$$

which contains two unitary operators that describe the effect of the kick and the propagation in between two kicks, respectively ($\hat{p}$ and $\hat{q}$ denote the position and momentum operators).

Because of the classical periodicity in both p and q, we can consider tunneling between the main regular island centered around $(p,q) = (0,0)$ and its counterparts that are shifted by integer multiples of 2π along the momentum axis or along the q-axis. To mimic a double-well configuration, we will restrict the boundary conditions for the eigenstates of $\hat{U}$ and consider tunneling between two islands centered around (i) $(p,q) = (0,0)$ and $(2\pi,0)$ or around (ii) $(p,q) = (0,0)$ and $(0,2\pi)$. The effective parity that allows to discriminate the eigenphases $\varphi_n^{\pm}$ of $\hat{U}$ manifests as $\tilde{\psi}_n^{\pm}(p+2\pi) = \pm\tilde{\psi}_n^{\pm}(p)$ for the corresponding eigenstates in momentum representation in case (i) and as $\psi_n^{\pm}(q+2\pi) = \pm\psi_n^{\pm}(q)$ for the eigenstates in position representation in case (ii). In both cases, tunneling will be characterized by the splitting

$$\Delta\varphi_n = |\varphi_n^{+} - \varphi_n^{-}| . \tag{8.69}$$

Numerically, it can be convenient to deal a finite Hilbert space of (even) size N, and this can be obtained provided the two phase space translation operators $\hat{T}_1 = \exp(2\pi i\hat{p}/\hbar)$ and $\hat{T}_2 = \exp(-2\pi i\hat{q}/\hbar)$ commute, which is the case if we choose $\hbar = 2\pi/N$ [57, 58].

8.4.2 Numerical computation of the eigenphase splittings

Figure 8.6 shows the eigenphase splittings $\Delta\varphi_0$ [see Eq. (8.69)] in case (ii) (tunneling in position) for the local "ground state" ($n = 0$) in the central island of the kicked rotor, i.e. for the state that is most strongly localized around the center of the island, at $K = 2.28$. While on average these splittings decrease exponentially with $1/\hbar$, significant fluctuations arise on top of that exponential decrease. In particular, large spikes are visible. As illustrated in Fig. 8.6b, they can be related to the crossing of "excited states" within the island, which are coupled to the ground state by a classical resonance. Fig. 8.6c shows the Husimi distribution of the relevant states involved, demonstrating that the coupling process is most effective when the states are symmetrically located on each side of the classical resonance. To illustrate that the influence of the resonances inside the regular islands is actually independent of the details of the chaotic regime (a major feature of the resonance-assisted and chaos-assisted tunneling schemes) we furthermore plot in Fig. 8.7 a comparison between the splittings for

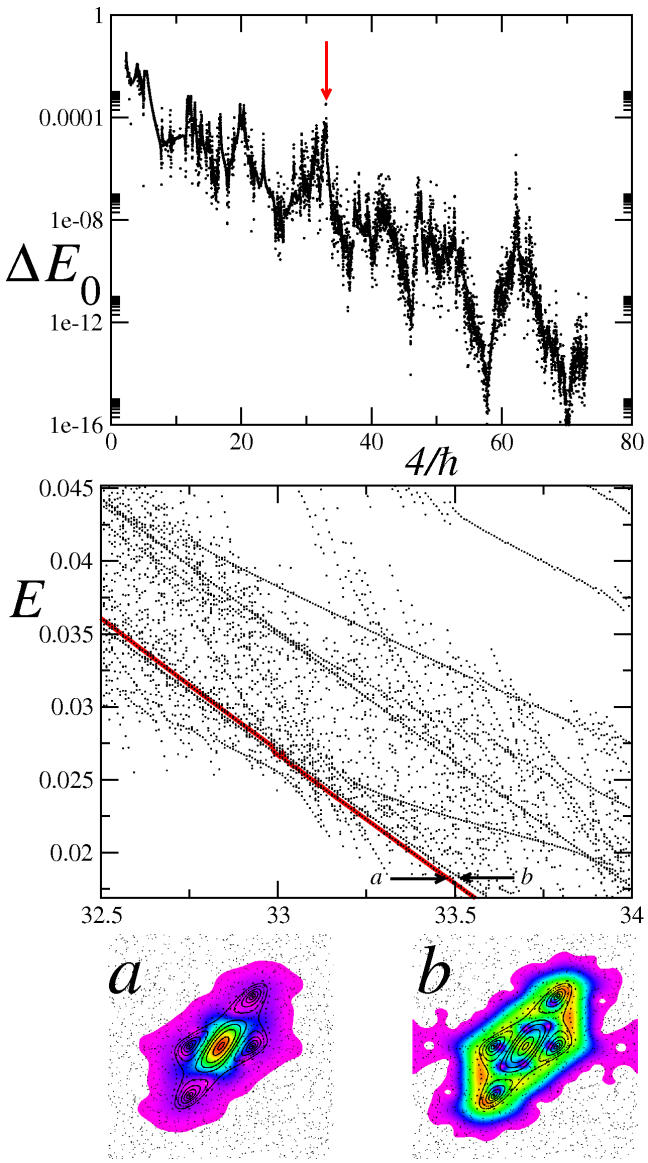

Figure 8.6: The upper panel shows the quasi-energy splittings in $\Delta E_0 = \hbar\varphi_0$ in the kicked rotor model for $K = 2.28$, corresponding to a $4:1$ classical resonance. Here we are concerned with a tunneling in q. The middle panel shows the quasi-energy spectrum $E_n^{\pm} = \hbar\varphi_n^{\pm}$ of $\hat{U}$ where only states with a significant overlap with a coherent state localized around $(p, q) = (0, 0)$ have been retained. The horizontal arrow a) marks the central state doublet ($n = 0$, not resolved at that scale) and the arrow b) indicates the third excited state localized in the island ($n = 4$). Their Husimi distribution superimposed with the Poincaré surface of section are shown in the lower panel in order to illustrate the clear correspondence between the classical and the quantum resonance. As $1/\hbar$ increases, the crossing of the doublet by the resonant state provokes the large and wide spike indicated by the vertical arrow in the upper panel.

the cases (i) and (ii) of tunneling in p and q direction, respectively. The (rough) matching between the dominant spikes of fluctuations in both cases confirms that tunneling outside one island is mainly isotropic in phase space.

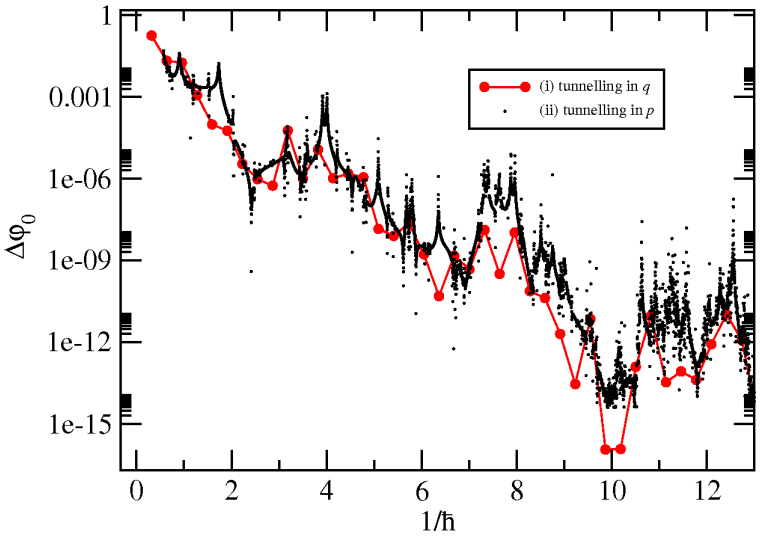

Figure 8.7: Comparison between the splitting $\Delta\varphi_0$ for the kicked rotor at $K = 2$ for (i) the case of tunneling between two islands centered at $(p, q) = (0, 0)$ and at $(p, q) = (2\pi, 0)$, and (ii) the case of tunneling between two islands centered at $(p, q) = (0, 0)$ and at $(p, q) = (0, 2\pi)$. In this latter case, we restricted ourselves to even integer values of $N = 2\pi/\hbar$ for which the splittings can be computed by diagonalizing finite $N \times N$ matrices beyond the double precision.

From now on, we will consider case (i) only (tunneling in momentum) with $N = 2\pi/\hbar$ being an integer, corresponding to the number of Planck cells that fit into one Bloch cell. Figures 8.9 and 8.10 show the eigenphase splittings $\Delta\varphi_0$ of the island's ground state for $K = 2.6, 2.8, 3.0$ (Fig. 8.9) as well as for $K = 3.2, 3.4, 3.6$ (Fig. 8.10). As in Refs. [31, 32], these splittings were calculated with a diagonalization routine for complex matrices that is based on the GMP multiple precision library [59], in order to obtain accurate eigenvalue differences below the ordinary machine precision limit.

8.4.3 Semiclassical calculations

The role played by the nonlinear resonances in the tunneling mechanism is made explicit by comparing these numerically calculated splittings with semiclassical predictions based on the most relevant resonances that are encountered in phase space. In practice, we took those r:s resonances into account that exhibit the smallest possible values of r and s for the winding numbers s/r under consideration. In all of the considered cases, the "quantum boundary" of the regular island, which determines the value of k_c through Eq. (8.40), was defined by the partial barrier that results from the intersections of the inner stable and unstable manifolds associated with the hyperbolic periodic points of the 4:1 resonance (see also Fig. 8.5). While this partial barrier lies rather close to the classical chaos border of the island for $K = 2.6$ (Fig. 8.9), it encloses an appreciable part of the chaotic sea for $K = 3.6$ (Fig. 8.10) including

some relevant nonlinear resonances.

Pure resonance-assisted tunneling

We stress that the semiclassical calculations shown in Figs. 8.9 and 8.10 involve a few differences as compared to some of our previous publications [31, 32, 33, 34]. To start with, (I) the action dependence of the coupling coefficients associated with the resonances has been included [see Eq. (8.36)]. Furthermore, the unperturbed energy differences $E_n - E_{n+kr}$ of the quasi-modes are not computed via the quadratic pendulum approximation (8.24). Instead, as illustrated on Fig. 8.8, (II) a global parabolic fit to the action dependence of the frequency $\Omega \equiv \Omega(I)$ was applied on the basis of the classically computed values of the resonant actions $I_{r:s}$ and their frequencies $\Omega(I_{r:s}) = (s/r)\,\omega$, for a sequence of resonances with not too large r and s. Theses two modifications significantly improve the reproduction of individual peak structures in the tunneling rates.

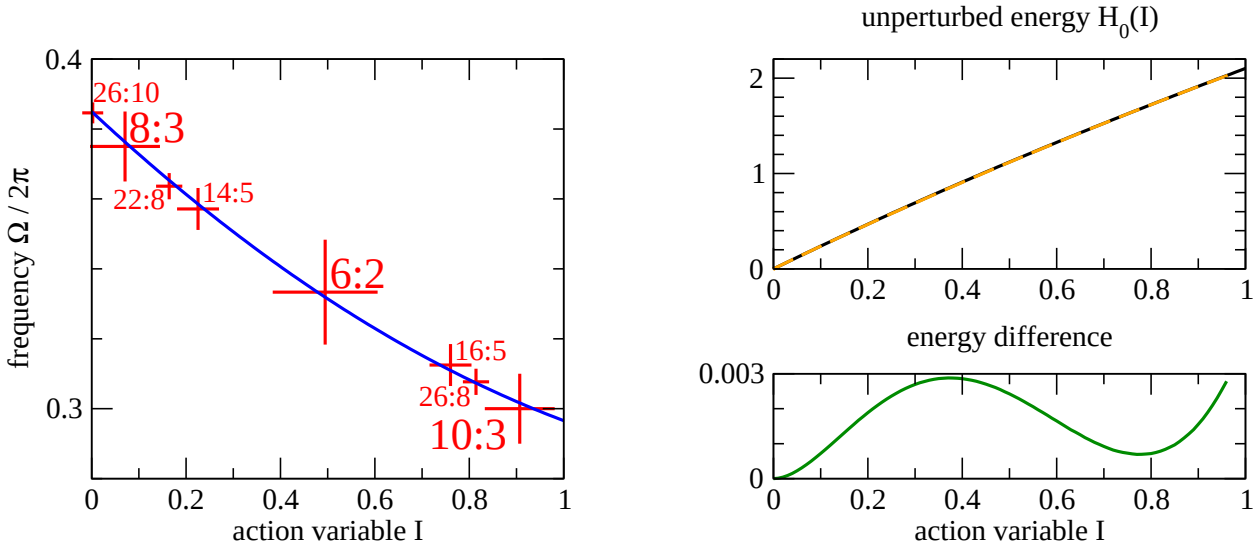

Figure 8.8: Unperturbed energies and oscillation frequencies within the regular island of the kicked rotor at $K = 3.5$. The left panel shows the action dependence of the oscillation frequencies as computed from a quadratic fit to individual nonlinear resonances (crosses), which results in the expression $\Omega(I) = 2.41886 - 0.790561I + 0.235191I^2$ (solid line). The upper right panel compares the unperturbed energies resulting from the integration of this quadratic expression (solid line) with the unperturbed energies used in Ref. [35] that were obtained by analyzing a dense set of quasi-periodic trajectories within the regular island (dashed line) [60]. This latter approach yields $\Omega(I) = 2.41740 - 0.952917I + 1.00151I^2 - 1.00153I^3 + 0.368829I^4$, which essentially constitutes the definition of the fictitious integrable system used in Ref. [35]. Although the difference between these two approaches is rather small as shown in the lower right panel, it plays a significant role for the tunneling rates in the deep semiclassical limit (see Fig. 8.12).

With these improvements (I) and (II), we generally find that the quantum splittings are quite well reproduced by our simple semiclassical theory based on nonlinear resonances. In particular, the location and height of prominent plateau structures and peaks in the

tunneling rates can, in almost all cases, be quantitatively reproduced through resonance-assisted tunneling. The additional fluctuations of the splittings on a small scale of N, however, cannot be accounted for by our approach as they arise from the details of the eigenspectrum in the chaotic block of the Hamiltonian. Their average size, however, seems in good agreement with the universal prediction (8.64) for the variance of eigenphase splittings in chaos-assisted tunneling.

Note that there is a general tendency of the semiclassical theory to overestimate the exact splittings wherever the latter encounter local minima. We attribute those minima to the occurrence of destructive interferences between different pathways that connect the ground state to a given excited state $|n\rangle$. As pointed out in the discussion of Eq. (8.41), such destructive interferences are not yet accounted for in our present implementation of resonance-assisted tunneling. Their inclusion would require to take into account the phases ϕ_k associated with individual resonances [see Eq. (8.13)], the discussion of which is beyond the scope of this article.

Resonance-assisted tunneling at a bifurcation

As a last comment, we note that the influence of a nonlinear resonance on tunneling processes in mixed systems may persist even if that resonance is not at all manifested in the classical phase space. This is precisely the case at the value of the perturbation parameter at which this resonance is bifurcating from the center of the island, i.e., at which the central fixpoint of the island exhibits a rational winding number corresponding to the resonance under consideration. A prominent example in the kicked rotor model is found at $K = 2$ where the central fix point has the winding number 0.25. Indeed, $K = 2$ is exactly the critical value where two periodic orbits of period 4 coalesce in the center, both separately coming from the complex phase space (their action being strictly negative for $K < 2$) and then becoming real and distinct (one stable and one unstable) for $K > 2$.

Following the normal-form arguments in Section 8.2.3, the scaling of the "classical size" of the resonance with the perturbation parameter K is, in lowest order, provided by the effective pendulum matrix element $V_{r:s}(K) = \tilde{v}_1[I_{r:s}(K)]^{rk/2}$ where $I_{r:s}(K)$ represents the dependence of the resonant action on K. However, as can be seen in Eq. (8.36), the associated coupling matrix elements that affect tunneling only depend on the prefactor $\tilde{v}_1$, which ought to be a well-behaved function of K showing no singular behaviour at the bifurcation point. Therefore, we have to conclude that these matrix elements remain finite even for $K \lesssim 2$.

This expectation is confirmed in Fig. 8.11, which shows the tunneling rates in the kicked rotor for $K = 2$. For this value, the only major resonance that is manifested in the classical phase space is the 10:2 resonance whose island chain is located near the boundary of the main island. Taking into account this resonance alone (as well as combining it with other resonances of higher order, the result of which is not shown in Fig. 8.11) apparently leads to a very strong underestimation of the quantum eigenphase splittings (in contrast to Ref. [31] where the action dependence of the coupling matrix elements was not properly incorporated). But once we take into account the 4:1 resonance and compute its corresponding classical parameters from the classical phase space at $K = 2.001$, we obtain a good reproduction of the quantum splittings.

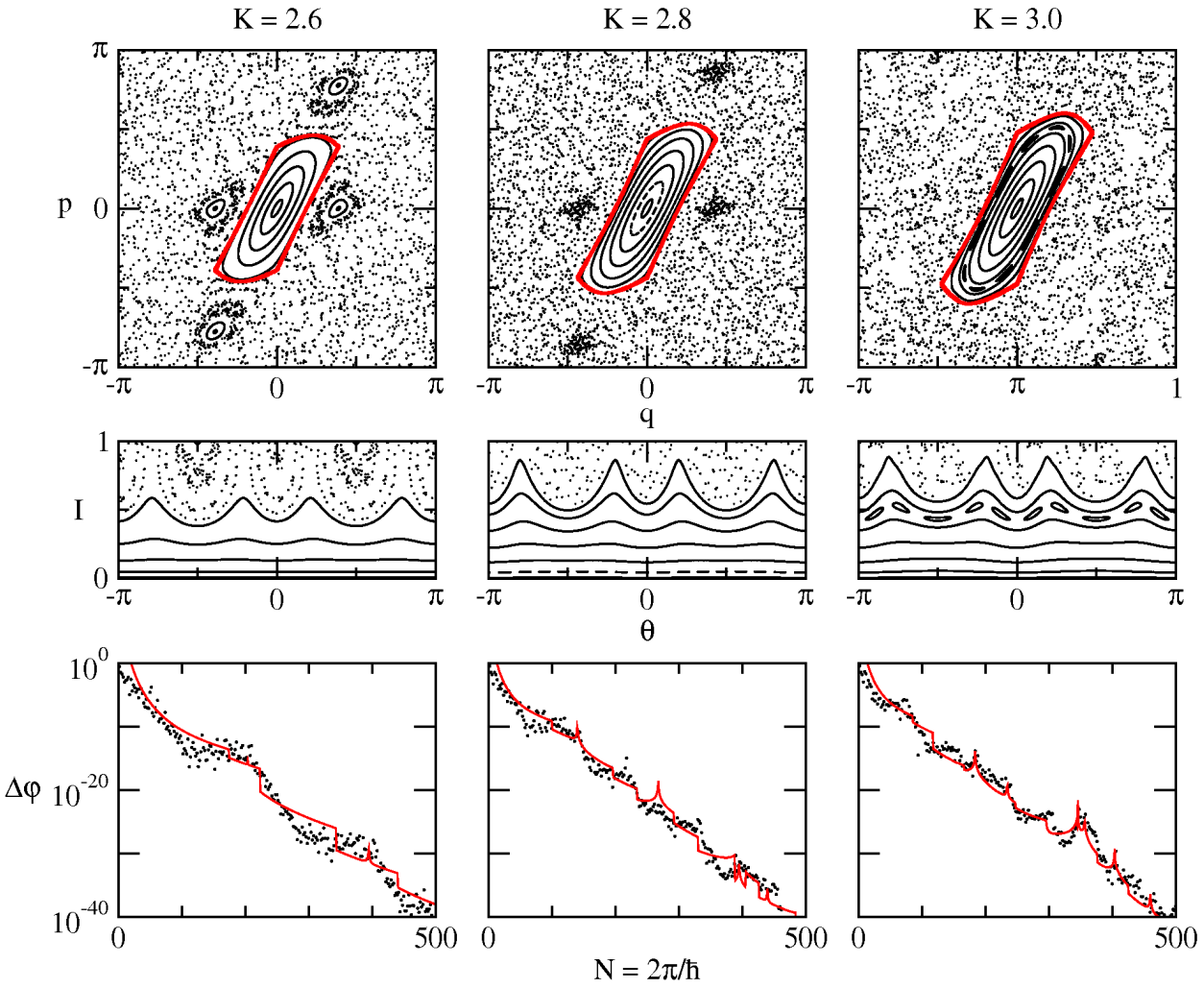

Figure 8.9: Quantum and semiclassical splittings in the kicked rotor model for $K = 2.6$ (left column) $K = 2.8$ (central column), and $K = 3$ (right column). The upper and middle panels show the classical phase space in the original phase space variables p and q, with the thick curve marking the effective quantum boundary of the island, and in approximate action-angle variables I and θ. The lower panels display the quantum and semiclassical eigenphase splittings (dots and solid lines, respectively) of the ground state in the central regular island. For the semiclassical splittings, we used the 14:4 and 18:5 resonances for $K = 2.6$, the 10:3 and 14:4 resonances for $K = 2.8$, and the 10:3, 14:4, 16:5, and 22:7 resonances for $K = 3$. As pointed out in the text, the splittings were computed with a generalization of the multi-resonance expression (8.41) to mixed systems, using (I) the corrected action dependence (8.36) of the matrix elements and (II) unperturbed energies that were determined from a global parabolic fit of $\Omega(I)$, and (III) computing the coupling to the chaotic domain via the outermost nonlinear resonance, as explained at the end of section 8.3.5. The discontinuous steps in the semiclassical splittings are actually induced by the discontinuity of the integer part in the expression (8.40) for the maximal number k_c of couplings within the island.

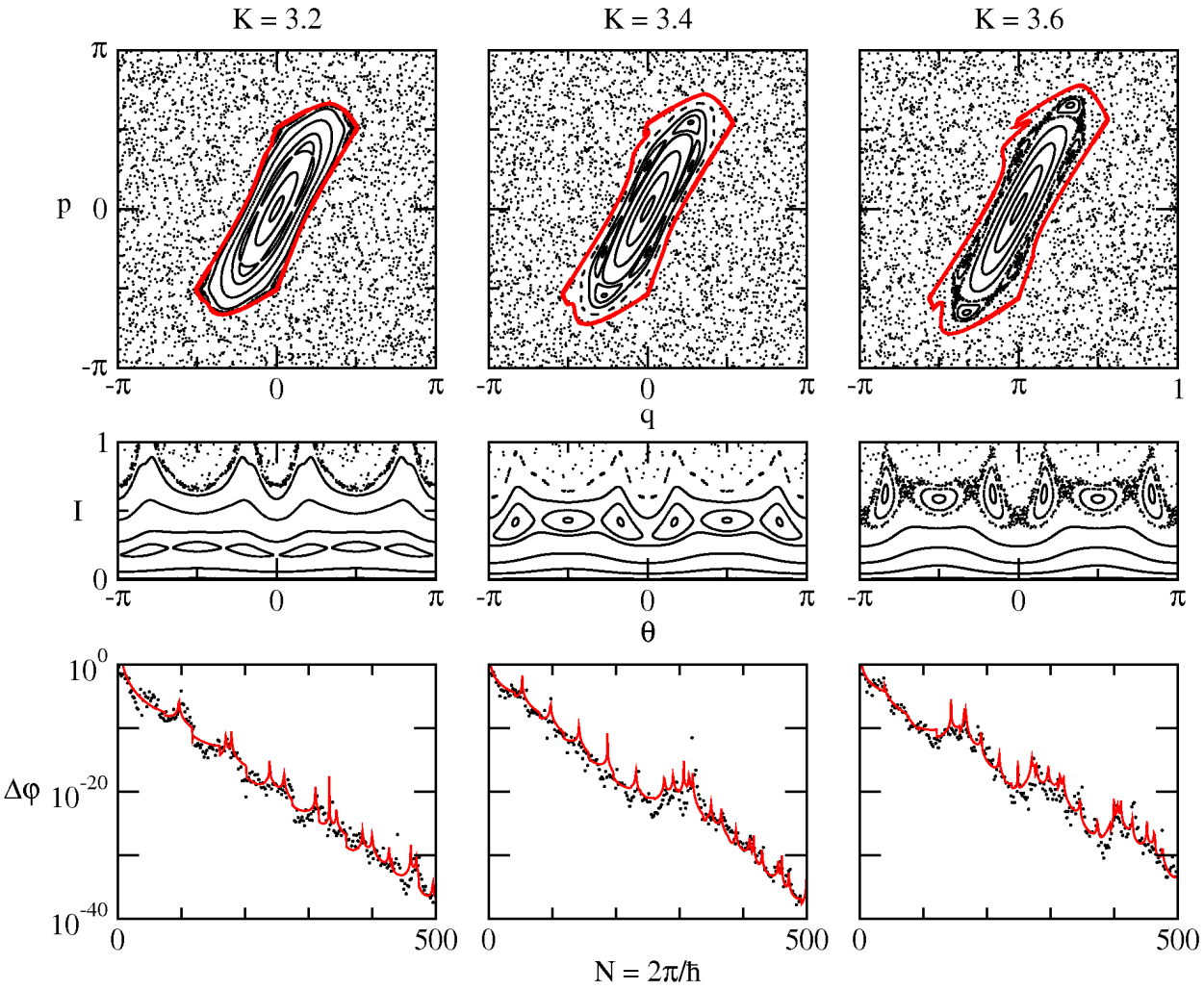

Figure 8.10: Same as Fig. 8.9 for $K = 3.2$, $K = 3.4$, and $K = 3.6$. For the semiclassical splittings, we used the 6:2 and 10:3 resonances for $K = 3.2$, the 6:2, 10:3, and 14:5 resonances for $K = 3.4$, and the 6:2 and 8:3 resonances for $K = 3.6$.

Combination with direct regular-to-chaotic couplings

In the semiclassical predictions shown in Figs. 8.9, 8.10, and 8.11, we have, following the discussion in section 8.3.4, assumed that the resonance-assisted mechanism was providing the relevant couplings not only within the regular island, but also (III) from the edge of the regular island to the chaotic sea. As pointed out in section 8.3.2, the regular-chaos boundary is, however, the place where approximation schemes are not controlled any longer. It is therefore useful to compare the results obtained in this way with those derived from the more precise evaluation of the direct regular-chaotic couplings (IIIb) computed with Eq. (8.45) through a numerical application of the quantum evolution operator $\hat{U}$.

Figure 8.12 shows the resulting comparison for the eigenphase splittings of the quantum

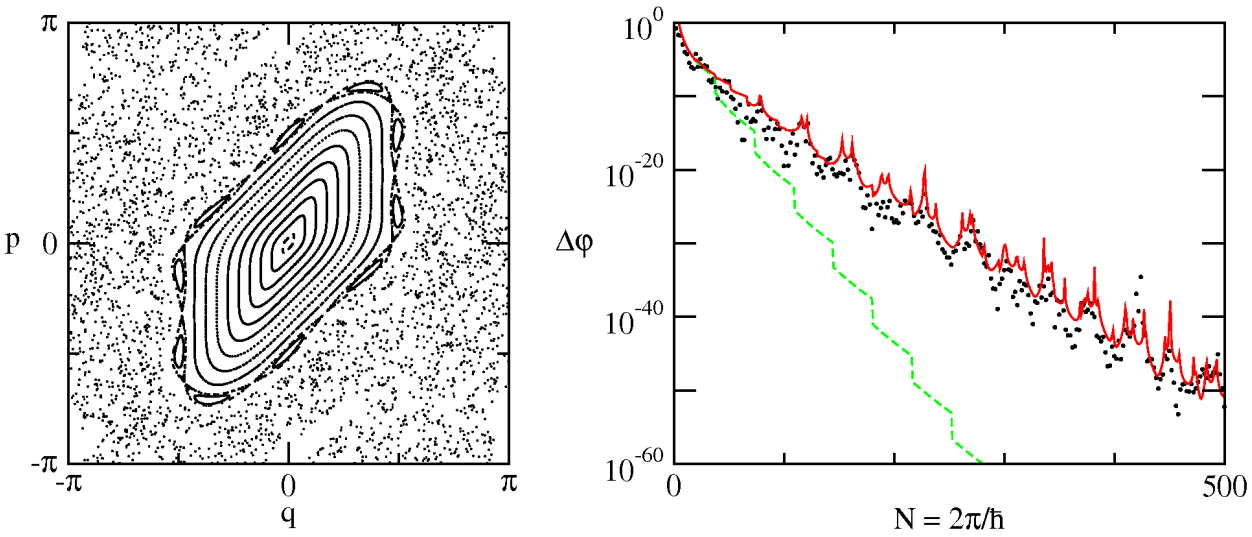

Figure 8.11: Resonance-assisted tunneling in the kicked rotor at a bifurcation. The left panel shows the classical phase space for $K = 2$, which contains a prominent 10:2 resonance close to the border of the island, and the right panel displays the corresponding quantum eigenphase splittings (dots). Semiclassical calculations of the splittings (solid and dashed lines, using the same levels of approximation as in Figs. 8.9 and 8.10) were carried out using the 10:2 resonance only (dashed line) as well as a combination of the 4:1 resonance and the 10:2 resonance, the former emerging at the island's center right at $K = 2$. The parameter $\tilde{v}_1$ associated with that 4:1 resonance [see Eq. (8.36)] was determined from the classical phase space at $K = 2.001$.

kicked rotor at $K = 3.5$ [35] (see Fig. 8.3 for the corresponding classical phase space). In addition to the quantum and semiclassical splittings obtained in the same way as in Figs. 8.9 and 8.10 (black and red curves, respectively), two additional curves are shown. The green one corresponds to a fully semiclassical calculation for which the regular-to-chaotic couplings are evaluated by the resonance-assisted mechanism. In contrast to the red curves and to the calculations in Figs. 8.9 and 8.10, however, the action dependence $H_0(I)$ of the unperturbed energies within the island was not obtained by a fit to several relevant resonances as described above, but rather (IIb) by computing the action and the rotation number for a dense set of trajectories within the island, from which the energies are deduced via the relation $\Omega(I) = dH_0(I)/dI$ [60] (see, e.g., Fig. 11 of Ref. [11] and the associated text for a detailed discussion). The blue curve implements, in addition to these improved energies, an evaluation of the direct regular-chaotic coupling (IIIb) using the approach of Bäcker et al. [22] [see Eq. (8.45)]; it actually corresponds to the curve published in Fig. 3 of Ref. [35].

What is observed in Fig. 8.12 is that, although there is good agreement between the three theoretical curves and the numerical one for a large range of $N = 2\pi/\hbar$, some significant deviations arise in the range $300 < N < 450$. Remarkably, however, the most striking discrepancies that are encountered for the red curve (i.e., for the full semiclassical calculation *without* the improved energies) are essentially cured once the improved energies are implemented (green curve). Adding the semi-numerical evaluation of the direct regular-to-chaotic coupling further improves the prediction, but to a significantly lesser degree.

Figure 8.8 compares $H_0(I)$ computed for the kicked rotor at $K = 3.5$ by the two methods

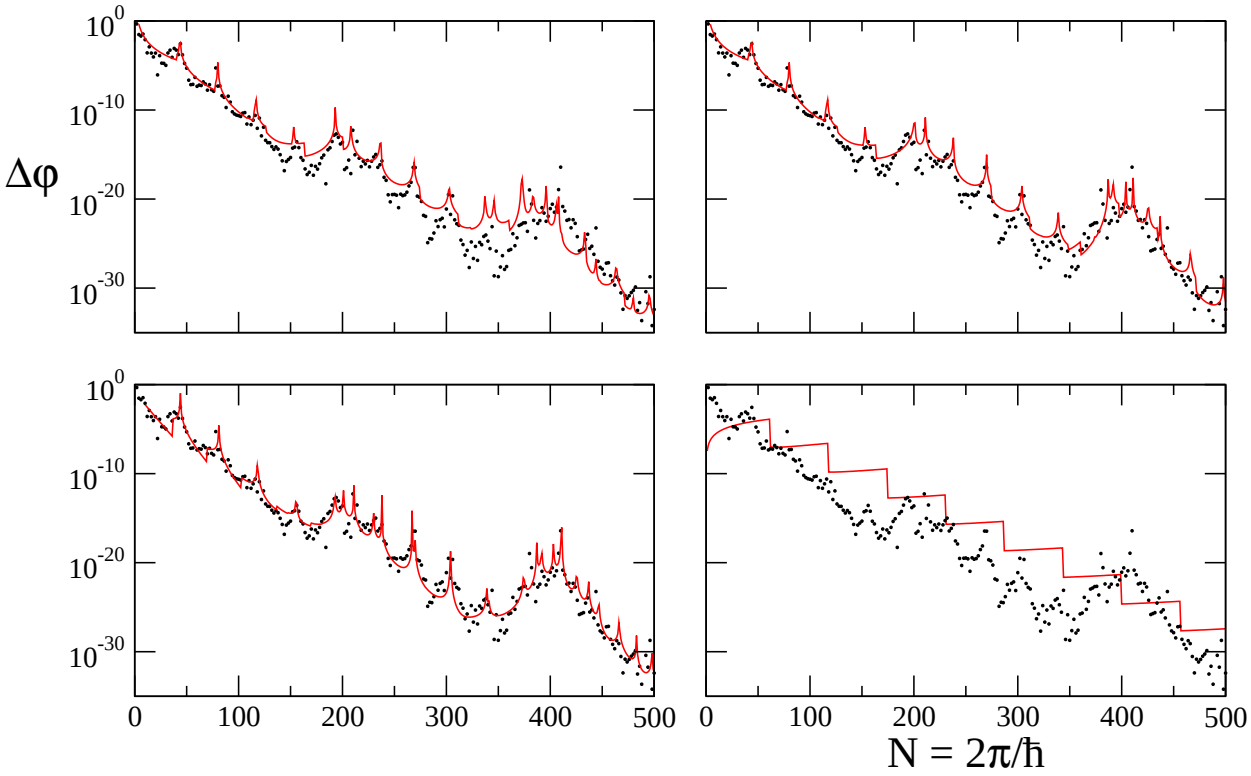

Figure 8.12: Quantum and semiclassical splittings in the kicked rotor model for $K = 3.5$ (see Fig. 8.3 for the classical phase space). As in Figs. 8.9 and 8.10, the dots and solid lines represent, respectively, the quantum splittings and the semiclassical prediction. In the upper left panel, this prediction is based on our approach, where we take into account the 6:2, 8:3, 10:3, and 14:5 resonances. The upper right panel shows the same calculation, except that a more refined evaluation of the unperturbed energies (and their action dependence) is used (IIb) (see text and Fig. 8.8). The lower left panel shows the prediction that is obtained with these improved energies and with an evaluation of the direct regular-chaotic coupling (IIIb) using the fictitious integrable system approach of Bäcker et al. [22] [which amounts to applying the quantum kicked rotor map onto the corresponding eigenstate of the integrable system, see Eq. (8.45)]. Finally, the lower right panel shows the prediction that would be obtained with the 6:2 resonance according to the approach outlined in Ref. [31], i.e. neglecting the action dependence of the coupling matrix elements, neglecting the occurence of partial barriers in the chaotic domain, and making a simple quadratic expansion of the unperturbed energies in the vicinity of the resonance.

under consideration, namely the fitting approach using the most relevant resonances (which is illustrated in the left panel of Fig. 8.8) and the more refined approach based on a dense set of trajectories [60]. Apparently, both approaches yield nearly identical energies, with relative differences being well below one percent (see the lower right panel of Fig. 8.8). This underlines that small imprecisions in the prediction of the unperturbed eigenenergies of regular quasi-modes may, under special conditions, lead to dramatic over- or underestimations of the tunneling rates in mixed systems. In the particular case considered here, it seems to be the transition across the 8:3 resonance, located rather close to the center of the island, which is not properly described using the more approximate energies. This gives rise to a horizontal

shift of the predicted splittings towards smaller N, as is clearly seen in Fig. 8.12. This issue obviously requires further investigations. It does, however, not seem to put into question the principal conclusion that the resonance-assisted coupling mechanism provides an accurate approach to evaluate regular-to-chaotic tunneling rates in a purely semiclassical manner.

8.5 Conclusion

In summary, we have provided a comprehensive description of the theory of resonance-assisted tunneling in mixed regular-chaotic systems. This description is partly based on previous publications of ours [27, 28, 31, 32, 33], but contains also some new aspects and significant improvements especially concerning the determination of the matrix elements associated with resonance-induced couplings. Moreover, partial barriers in the chaotic domain are now incorporated into the scheme of resonance-assisted tunneling, which generally gives rises to an effective enhancement of the size of the regular islands under consideration. In practice, we find that the most relevant partial barriers for tunneling are constituted by combinations of stable and unstable manifolds that are associated with hyperbolic periodic points of low-order nonlinear resonances within the chaotic domain. The application of this approach to the kicked rotor model yields rather good agreement between the "exact" eigenphase splittings of states that are localized in the center of the main regular island, and their semiclassical predictions based on nonlinear resonances.

The main message that we intend to communicate here is that resonance-assisted tunneling not only allows one to understand the origin of plateaus and peak structures, in the tunneling rates. It also provides a simple, readily implementable scheme to quantitatively predict the appearance of such structures on the basis of purely classical information. In practice, one needs for this purpose to identify the relevant resonances in the regular phase space region under consideration, to find their stable and unstable fixpoints in the Poincaré surface of section, to compute their stability indices and the areas enclosed by their separatrix structures, respectively by their stable and unstable manifolds, and finally to compute the flux enclosed by the turnstiles in order to determine effective "quantum chaos border" of the island. Even for a simple model like the kicked rotor, this programme requires much less numerical effort than a quantum calculation of the tunneling rates. As we demonstrated for the kicked rotor, it provides, on the other hand, a reproduction of the quantum tunneling rates which is extremely satisfactory from a quantitative point of view. This numerical accuracy requires, however, a careful evaluation of the various classical parameters entering into the semiclassical calculation of the splittings. This includes the action dependence of the resonance-Hamiltonian couplings, the effective size of the regular island, and the evaluation of the unperturbed energies within the island. It turns out in particular that in some circumstances, e.g. at $K = 3.5$ in the range $300 < N < 450$, very small imprecision in the determination of the unperturbed eigenenergies may significantly affect the accuracy of the semiclassical predictions.

We expect that the framework of resonance-assisted tunneling can be generalized to systems with more than two effective degrees of freedom, although the identification of important resonances might become more involved in such systems and resonance-assisted (quantum) tunneling might compete there with (classical) Arnol'd diffusion in the deep semiclassical regime [30]. Another open problem which needs to be addressed in more detail concerns the role of nonlinear resonances in trajectory-based semiclassical approaches to tunneling, put forward by Shudo, Ikeda, and coworkers [36, 37, 38] (see also the corre-

sponding chapters in this book), which involve the complexified classical phase space and are more rigorous from a formal semiclassical point of view than our approach. We strongly believe that nonlinear resonances should leave their characteristic traces in the self-similar complex phase space structures that govern tunneling in this framework [36, 37]. Such an insight should significantly contribute to rendering those approaches practicable for more complicated systems as well — and underline the semiclassical nature of resonance-assisted tunneling.

Acknowledgements

We are grateful to Olivier Brodier, Dominique Delande, Christopher Eltschka, Kensuke Ikeda, Jérémy Le Deunff, Steffen Löck, Srihari Keshavamurthy, Roland Ketzmerick, Mirjam Schmid, Akira Shudo and Steve Tomsovic for helpful assistance and stimulating discussions. We furthermore acknowledge financial support by the Deutsche Forschungsgemeinschaft (DFG) through the Forschergruppe FOR760 “Scattering systems with complex dynamics”.

References

[1] M. J. Davis and E. J. Heller, J. Chem. Phys. **75**, 246 (1981).
[2] W. K. Hensinger, H. Häffner, A. Browaeys, N. R. Heckenberg, K. Helmerson, C. McKenzie, G. J. Milburn, W. D. Phillips, S. L. Rolston, H. Rubinsztein-Dunlop, and B. Upcroft, Nature **412**, 52 (2001).
[3] D. A. Steck, W. H. Oskay, and M. G. Raizen, Science **293**, 274 (2001).
[4] A. Mouchet, C. Miniatura, R. Kaiser, B. Grémaud, and D. Delande, Phys. Rev. E **64**, 016221 (2001).
[5] C. Dembowski, H.-D. Gräf, A. Heine, R. Hofferbert, H. Rehfeld, and A. Richter, Phys. Rev. Lett. **84**, 867 (2000).
[6] S. Creagh, in *Tunneling in Complex Systems*, edited by S. Tomsovic (World Scientific, Singapore, 1998), pp. 1–65.
[7] L. D. Landau and E. M. Lifshitz, *Quantum Mechanics: Non-Relativistic Theory* (Pergamon, Oxford, 1958).
[8] S. C. Creagh, J. Phys. A **27**, 4969 (1994).
[9] W. A. Lin and L. E. Ballentine, Phys. Rev. Lett. **65**, 2927 (1990).
[10] O. Bohigas, D. Boosé, R. Egydio de Carvalho, and V. Marvulle, Nucl. Phys. A **560**, 197 (1993).
[11] O. Bohigas, S. Tomsovic, and D. Ullmo, Phys. Rep. **223**, 43 (1993).
[12] S. Tomsovic and D. Ullmo, Phys. Rev. E **50**, 145 (1994).
[13] E. Doron and S. D. Frischat, Phys. Rev. Lett. **75**, 3661 (1995).
[14] S. D. Frischat and E. Doron, Phys. Rev. E **57**, 1421 (1998).
[15] A. Ishikawa, A. Tanaka and A. Shudo, Phys. Rev. E **80**, 046204 (2009).
[16] F. Grossmann, T. Dittrich, P. Jung, and P. Hänggi, Phys. Rev. Lett. **67**, 516 (1991).
[17] F. Leyvraz and D. Ullmo, J. Phys. A **29**, 2529 (1996).
[18] A. Mouchet and D. Delande, Phys. Rev. E **67**, 046216 (2003).
[19] V. A. Podolskiy and E. E. Narimanov, Phys. Rev. Lett. **91**, 263601 (2003).
[20] V. A. Podolskiy and E. E. Narimanov, Opt. Lett. **30**, 474 (2005).
[21] A. Bäcker and R. Ketzmerick, private communication.
[22] A. Bäcker, R. Ketzmerick, S. Löck, and L. Schilling, Phys. Rev. Lett. **100**, 104101 (2008).
[23] A. Bäcker, R. Ketzmerick, S. Löck, M. Robnik, G. Vidmar, R. Höhmann, U. Kuhl, and H.-J. Stöckmann, Phys. Rev. Lett. **100**, 174103 (2008).
[24] A. M. Ozorio de Almeida, J. Phys. Chem. **88**, 6139 (1984).
[25] T. Uzer, D. W. Noid, and R. A. Marcus, J. Chem. Phys. **79**, 4412 (1983).
[26] L. Bonci, A. Farusi, P. Grigolini, and R. Roncaglia, Phys. Rev. E **58**, 5689 (1998).
[27] O. Brodier, P. Schlagheck, and D. Ullmo, Phys. Rev. Lett. **87**, 064101 (2001).
[28] O. Brodier, P. Schlagheck, and D. Ullmo, Ann. Phys. **300**, 88 (2002).
[29] S. Keshavamurthy, J. Chem. Phys **122**, 114109 (2005).
[30] S. Keshavamurthy, Phys. Rev. E **72**, 045203(R) (2005).
[31] C. Eltschka and P. Schlagheck, Phys. Rev. Lett. **94**, 014101 (2005).
[32] P. Schlagheck, C. Eltschka, and D. Ullmo, in *Progress in Ultrafast Intense Laser Science I*, edited by K. Yamanouchi, S. L. Chin, P. Agostini, and G. Ferrante (Springer, Berlin, 2006), pp. 107–131.
[33] A. Mouchet, C. Eltschka, and P. Schlagheck, Phys. Rev. E **74**, 026211 (2006).
[34] S. Wimberger, P. Schlagheck, C. Eltschka, and A. Buchleitner, Phys. Rev. Lett. **97**, 043001 (2006).
[35] S. Löck, A. Bäcker, R. Ketzmerick, and P. Schlagheck, Phys. Rev. Lett. **104**, 114101 (2010).
[36] A. Shudo and K. S. Ikeda, Phys. Rev. Lett. **74**, 682 (1995).
[37] A. Shudo and K. S. Ikeda, Phys. Rev. Lett. **76**, 4151 (1996).

[38] A. Shudo, Y. Ishii, and K. S. Ikeda, J. Phys. A **35**, L225 (2002).
[39] A. J. Lichtenberg and M. A. Lieberman, *Regular and Stochastic Motion* (Springer-Verlag, New York, 1983).
[40] S. Tomsovic, M. Grinberg, and D. Ullmo, Phys. Rev. Lett. **75**, 4346 (1995).
[41] G. D. Birkhoff, *Dynamical Systems* (Am. Math. Soc., New York, 1966).
[42] F. G. Gustavson, Astron. J. **71**, 670 (1966).
[43] A. M. Ozorio de Almeida, *Hamiltonian systems* (Cambridge University Press, 1988)
[44] P. Leboeuf and A. Mouchet, Ann. Phys, **275**, 54 (1999).
[45] E. Merzbacher, *Quantum mechanics*, 2nd ed. (Wiley, New York, 1970).
[46] R. E. Langer, Phys. Rev. **51**, 669 (1937).
[47] A. J. F. Siegert, Phys. Rev. **56**, 750 (1939).
[48] J. Le Deunff and A. Mouchet, Phys. Rev. E **81**, 046205 (2010).
[49] B. Chirikov, in *Chaos and Quantum Physics*, edited by M. J. Giannoni, A. Voros, and J. Zinn-Justin (North-Holland, Amsterdam, 1991), p. 201.
[50] D. Ullmo, Rep. Prog. Phys. **71**, 026001 (2008).
[51] O. Bohigas, S. Tomsovic, and D.Ullmo, Phys. Rev. Lett. **65**, 5 (1990).
[52] R. S. MacKay, J. D. Meiss, and I. C. Percival, Phys. Rev. Lett. **52**, 697 (1984).
[53] R. S. MacKay, J. D. Meiss, and I. C. Percival, Physica **13D**, 55 (1984).
[54] J. D. Meiss and E. Ott, Phys. Rev. Lett. **55**, 2742 (1985).
[55] N. T. Maitra and E. J. Heller, Phys. Rev. E **61**, 3620 (2000).
[56] R. Ketzmerick, L. Hufnagel, F. Steinbach, and M. Weiss, Phys. Rev. Lett. **85**, 1214 (2000).
[57] F. Izrailev and D. Shepelyansky, Sov. Phys. Dokl. **24**, 996 (1979).
[58] S. Fishman, I. Guarneri, and L. Rebuzzini, Phys. Rev. Lett. **89**, 084101 (2002).
[59] `http://gmplib.org`.
[60] We are indepted to Steffen Löck who carried out this calculation and sent us the resulting data.